UNIVERSITY OF CALIFORNIA,
IRVINE

Shrinkage Behavior of Polystyrene-based Foam Molded Parts Depending on Volatile Matter Content and Other Factors

THESIS

submitted in partial satisfaction of the requirements
for the degree of

MASTER OF SCIENCE

in Mechanical and Aerospace Engineering

by

Carineh Ghafafian

Thesis Committee:
Professor Kenneth D. Mease, Chair
Professor James C. Earthman
Professor Marc Madou

2016

Table of Contents

List of Tables

List of Figures

List of Abbreviations

EPS	Expanded polystyrene
EPE	Expanded polyethylene
EPP	Expanded polypropylene
PS	Polystyrene
TGA	Thermogravimetric analysis
DSC	Differential scanning calorimetry
T_g	Glass transition temperature
T_c	Crystallization temperature
T_m	Melting temperature
GC	Gas chromatography
MS	Mass spectrometry
GC	Gas chromatography
GC-MS	Gas chromatography/mass spectrometry
wt%	Weight percent
ESPI	Electronic speckle pattern interferometry
CCD	Charged couple device
SEM	Scanning electron microscopy
IPA	Isopropyl alcohol

Ackowledgements

It would not have been possible to write this Master Thesis without the help and support of the numerous kind people around me. Therefore, I would like to express my gratitude to the following people.

Above all, I would like to express the deepest appreciation to Professors Earthman, Mease, and Madou who gave me the opportunity to investigate this interesting theme and for their support as part of my thesis committee. I am thanking also Professor Atlstädt at the Department of Polymer Engineering at Universität Bayreuth, as well as the Particle Bead Foam Group at Neue Materialien Bayreuth GmbH for allowing me to collaborate with them on this topic. I am indebted there to my supervisor, Dipl.-Ing. Peter Schreier, and the technicians, Ute Kuhn and Max Löhner. I would also like to thank Dr. Christian Kuttner at the Leibniz Institute for Polymer Research and Matthias Burgard at the Universität Bayreuth Department of Macromolecular Chemistry II for their consistent assistance throughout the course of my research. I also place on record my sense of gratitude to one and all who, directly or indirectly, have lent me a helping hand at any point during this venture.

Last but not least, I would like to thank my family and friends (on both sides of the ocean) for constantly supporting me and being my biggest source of motivation during my studies. Especially I would like to thank my parents for their unparalleled encouragement and for giving me the opportunity to always pursue my interests.

Abstract of the Thesis

Shrinkage Behavior of Polystyrene-based Foam Molded Parts Depending on Volatile Matter Content and Other Factors

By

Carineh Ghafafian

Master of Science in Mechanical and Aerospace Engineering

University of California, Irvine, 2016

Professor Kenneth D. Mease, Chair

Polymer foam materials play a large role in the modern world. Expanded polystyrene (EPS) bead foam is a lightweight, low density, and good thermal and acoustic insulating material whose properties make it attractive for a number of applications, especially as building insulation. However, EPS also experiences post-molding shrinkage; it shrinks dimensionally from its molded size after processing. This means parts must be stored in warehouses until they are considered stable by the industry standard, DIN EN 1603. This often takes 11-18 weeks and is thus very timely and expensive. This study aims to decrease the post-molding shrinkage time of EPS foam by understanding the mechanisms of shrinkage behavior. Samples were split into two groups based on their amount of initial volatile matter content and storage conditions, then compared to a control group. Based on thermogravimetric analysis and gas chromatography with mass spectrometry, the volatile matter content and

composition was found to not be the sole contributor to EPS foam dimensional stability. Residual stress testing was done with the hole drilling method and Raman spectroscopy. As this type of testing has not been done with polymer foams before, the aim was to see if either method could reliably produce residual stress values. Both methods measured residual stress values with unknown accuracy. All samples stored at a higher temperature (60 °C) reached dimensional stability by the end of this study. Thus, air diffusion into EPS foam, encouraged by the high temperature storage, was found to play a significant role in post-molding shrinkage.

1 Introduction

1.1 Bead Foam Technology and Applications

Bead foams are unique materials, often based on commodity thermoplastics. They possess characteristics of low density and complex geometry capabilities [44, 53]. Only bead foams can have a high feasibility of free shape and, at the same time, maintain a very low density, even below 2% of the compact polymer [53]. Bead foams are made up of microgranular polymer beads expanded into foam particles with a blowing agent, then welded together with steam [53, 35]. The process of foaming generally begins with homogenization of the base polymer with a blowing agent, after which cells nucleate, grow, and stabilize in the melt. Cell stabilization is mainly affected by an increase in viscosity due to a decrease in temperature [35, 39, 53].

Bead foams can be classified by numerous factors, including cell size, cell population density (conventional, fine-celled, or microcellular), density, and cell structure. If cell walls remain intact during processing, the cell structure becomes closed-cell. This means that polymer cell wall layers separate each of the pockets of space between cells. Additionally, depending on the amount of expansion, blowing agent, and pre-foam process, the density can vary from very light (3-50 kg/m^3) to super-heavy (over 700 kg/m^3) [39]. They exhibit good impact resistance, energy absorption, insulation, heat resistance, and floatation. Thus, bead foams are used in a number of

applications, including building insulation, packaging, furniture, and automotive interiors [53].

1.2 EPS Properties and Applications

The current bead foam market consists of products made of three main base polymers. Expanded polystyrene (EPS) is the oldest of these, dating back to 1949. Expanded polyethylene (EPE) was the next to be introduced to the market in the 1970s, followed by expanded polypropylene (EPP) in the 1980s [39, 53].

EPS is a light, rigid foam with high impact resistance and good thermal insulation used in construction and packaging applications [24]. The basic units of EPS foam, micrograules, are into beads by steaming, in a pre-expander and then stabilized in silos under atmospheric conditions for 12-48 hours. As a slightly volatile, non-chlorofluorocarbon material, pentane is used as the blowing agent for EPS, and expands the compact microgranules into foam during processing. When pressure is released, the pentane blowing agent changes immediately to a vapor, which comes out of the solution with the polymer and thus expands the polymer microgranules into cellular beads, as shown below in *Figure 1*. The residual blowing agent then remains in the foam cells [39]. Lastly, the foam particles are steam-molded into bulk foam with a steam-chest molding machine [39, 53].

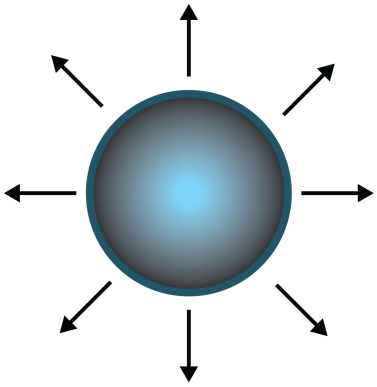

Figure 1: EPS beads expand when the pentane blowing agent turns into vapor from a release of pressure during processing. [Author]

EPS is among the biggest commodity polymers produced in the world. In 2014, its market value totaled $13.9 billion, and this number is expected to reach $22.4 billion by 2020 [5]. It is expected to make up 43% of the total volume of polymer foam market [6]. The largest share of the worldwide EPS demand is in Asia at 50%, as illustrated in *Figure 2*. Europe as the second-largest share takes approximately one quarter of the world's EPS [67].

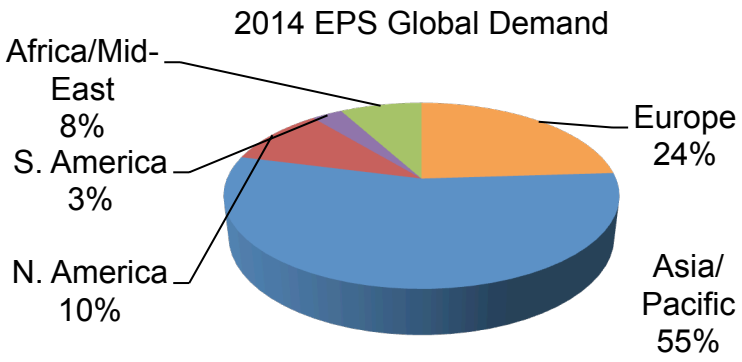

Figure 2: The breakdown of EPS global demand in 2014 based on region. [50]

The consumption and demand growth rates of EPS use have been increasingly positive since its introduction to the market half a century ago [6, 68]. In Asia, EPS consumption grew 110% between 2001 and 2011, and 60% in Europe in the same period, detailed in Table 1 [68]. Asia's new building insulation material regulations, as well as packaging, furniture, and automotive industry lightweight material requirements have driven this strong growth for polymer foam use in this region [6].

Table 1: EPS consumption growth in various regions of the world, from 2001 to 2011.
[Re-made from 68]

	Consumption (million tons)					
Region	**2001**	**2003**	**2005**	**2007**	**2009**	**2011**
Asia	1.447	1.903	1.943	2.330	2.493	3.079
Europe (incl. Russia)	1.118	1.100	1.266	1.624	1.614	1.801
North America	0.52	0.551	0.64	0.61	0.488	0.513
Rest of the world	0.168	0.211	0.25	0.347	0.382	0.44
Global consumption	**3.251**	**3.765**	**4.099**	**4.911**	**4.977**	**5.833**

The use of EPS throughout the world is predicted to continue to increase in the coming years. In Western Europe, 1.6% annual growth is anticipated for the next five years. In Asia, consumption of all polystyrene products is expected to grow over 3% annually for the next five years [7].

Being made up of 98% air and exhibiting low density and good sound absorption, EPS works well as lightweight thermal and acoustic insulation with consistent

performance, making it an attractive material [13, 39]. Due to increased requirements for thermal and sound insulation of new buildings as well as increased importance of bettering thermal insulation in old buildings, approximately 70% of EPS used in Europe is used in the construction industry, as illustrated in *Figure 3* [6, 24, 67]. Increase in overall wealth, industrial development in more regions of the world, as well as infrastructure investment will also continue to support the increasing market for EPS as an insulation material [6]. In Asia, large populations and increasing construction and packaging industry activities lead to higher EPS consumption because of its attractive properties [5].

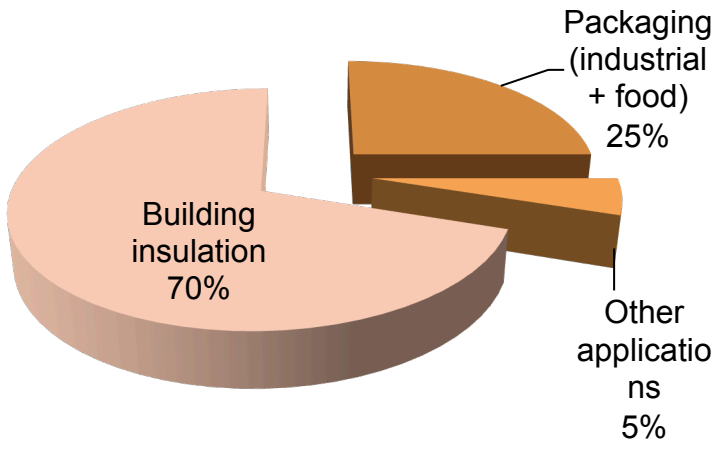

Figure 3: Applications of the EPS market in Europe. [Re-made, from 24]

Overall, the diverse range of applications leads to continuously high worldwide demand for EPS [67]. Over 100 companies around the world currently manufacture EPS. This number is expected to reach 200 within the next five years [5].

1.3 Research Motivation and Aims

Despite its highly attractive properties that make EPS one of the biggest commodity plastics in the world, the foam also experiences extensive post-molding shrinkage. This means it must be kept in storage for long durations of time before it can be utilized. If it is used before post-molding shrinkage is stabilized, it leads to highly problematic failures in numerous of its applications. For instance, as building insulation, EPS is installed as one of many layers that make up the building wall. The surrounding layer materials are specifically placed with respect to the size of the EPS boards at the time of insulation. Thus, if the EPS is not yet stable, it will continue to shrink in the coming weeks after installation. This will then cause the surrounding wall materials such as the mortar around brick, the adhesive holding materials together, as well as the wooden substrates to critically fail, ultimately leading to demolition of the entire wall. *Figure 4* below illustrates some of the surrounding materials to EPS in building insulation applications.

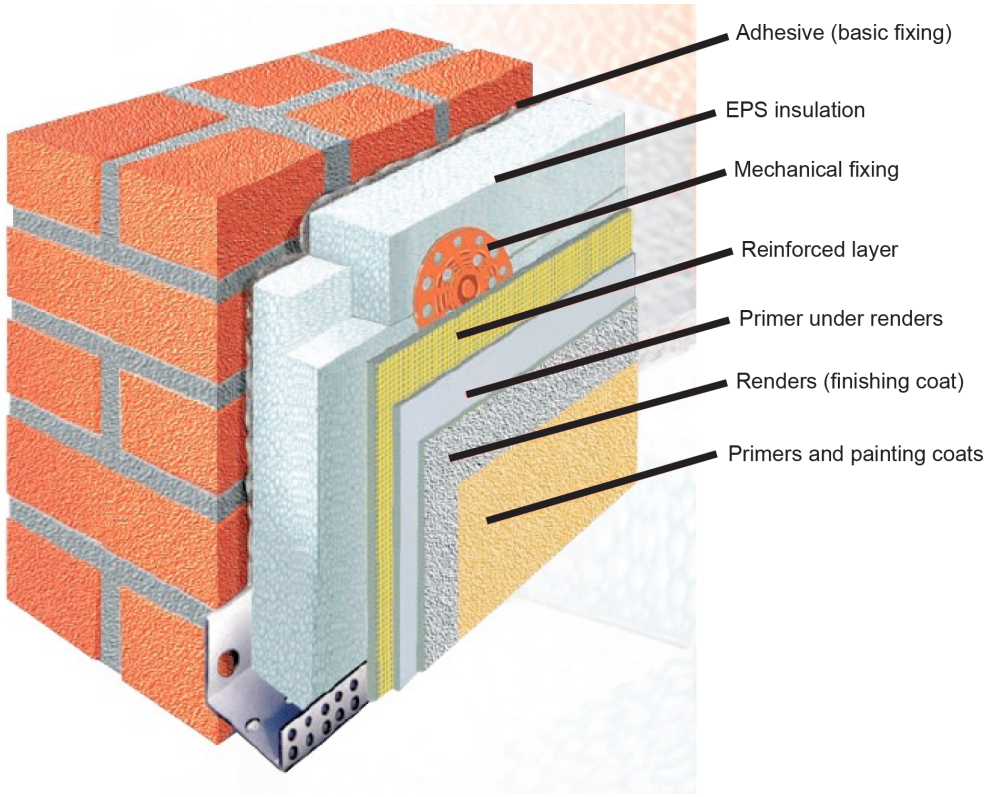

Figure 4: Building wall layers, showing materials that typically surround EPS in insulation applications. [Re-made from 11]

From an economic point of view, long-term storage of EPS is costly. The EPS foam beads are 40-60 times the volume of the original microgranules. Thus, the final EPS product takes up significantly more storage, shown below in *Figure 5*, inducing high warehouse charges.

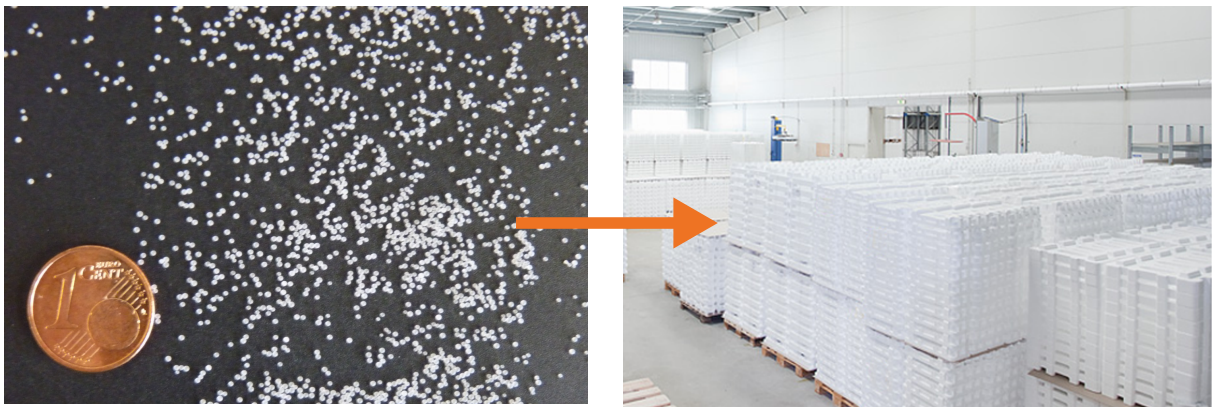

Figure 5: The difference in size of EPS raw material microgranules (left) versus final molded parts (right) after processing. This leads to the need for storage space, and thus high costs. The microgranules expnd 40-60 times in volume during processing. [24, 61]

The costly storage of EPS foam after processing is the motivation behind this study. In order to investigate the shrinkage behavior of EPS foam used in building insulation applications, DIN EN 1603 was adopted in this study. The industry-allowed shrinkage amount is defined by the standard, which states that EPS shrinkage is considered complete when the dimensional change between the last measurement and the measurement 28 days prior is less than 0.2%. This standard applies to EPS boards used in building insulation applications, which is a major use of the material throughout the world, especially in Europe. The dimensional change is defined as the percent difference between two measurements taken along the same axis, illustrated in Equation 1 below [62]. This benchmark set by DIN EN 1603 is often reached after 11-18 weeks of post-molding storage.

$$\%\, change = \frac{l_{x+28} - l_x}{l_x} \times 100 \qquad \textit{(Equation 1)}$$

EPS undergoes two known types of shrinkage after de-molding. De-molding is defined as removal of the EPS part from the mold after it is processed. Molding shrinkage takes place within the first 24 hours of de-molding, and is approximately the same in all directions and not more than 1% when stored at standard room temperature of approximately 20 °C [13, 44]. After the first 24 hours, the foam undergoes after-shrinkage, which is also approximately the same in all directions, but is affected by the material density, storage temperature, intermediate ageing duration, and the ageing of the finished product. After-shrinkage is hypothesized to occur mainly because of the loss of residual blowing agent, and low-pentane raw material products often exhibit less after-shrinkage [13]. *Figure 6* below illustrates the difference between the two types of shrinkage.

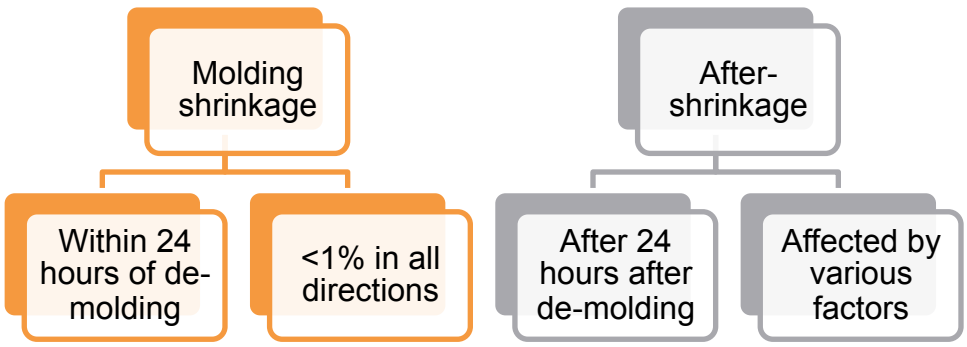

Figure 6: Two different types of shrinkage experienced by post-molded EPS foam. Understanding after-shrinkage (right) is the focus of this study. [Author]

When a partial vacuum develops inside foams cells because the structure is not strong enough to resist the excess pressure of atmosphere within the cells, after-

shrinkage occurs. This shrinkage is especially difficult to overcome in low-density, flexible, and semi-flexible closed-cell foams [35]. The focus of this study is to understand this after-shrinkage in EPS foam, as it takes a long amount of time and hence leads to very high storage costs of the foam molded parts after processing.

A number of factors are known to affect the duration of EPS foam after-shrinkage, including material density, storage temperature, intermediate aging duration, and residual blowing agent content [13, 35]. Additionally, materials often contain residual stresses because of cooling rates through the thickness of the mold after processing. When the mold is quickly cooled, the surface solidifies faster than the core. This causes shrinkage in the core with more cooling because of thermal contraction, but this shrinkage is constrained by the outer region that is already cooled, illustrated below in *Figure 7*. This can lead to undesirable residual stresses in the material that increase the likelihood of dimensional stability [42]. Thus, residual stresses, if present in the foam, could also be a factor in EPS shrinkage, but this has not been studied in great detail in prior literature and thus is not well known.

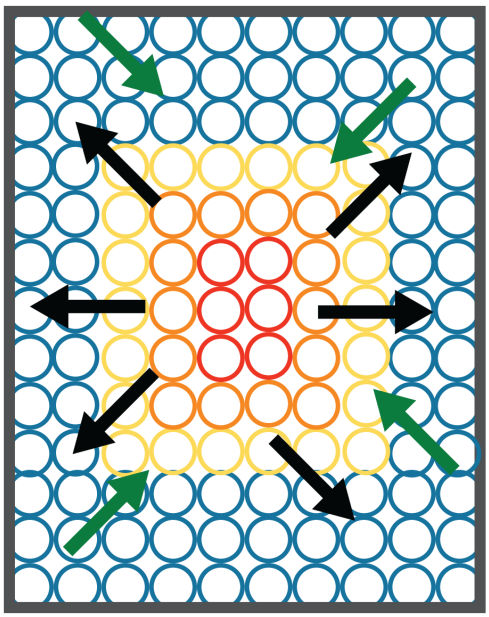

Figure 7: Simplified EPS cellular foam board showing possible residual stresses caused by processing. The black arrows signify tensile stresses, while the green arrows represent compressive stresses. [Author]

To reduce the costly and lengthy storage times of EPS, the main aim of this study is to fully understand the mechanisms of shrinkage behavior of EPS by the following means: 1) Construction of the correlation between the volatile content in the beads and shrinkage behavior; 2) Establish a method to measure the residual stresses in foams, since this has not been well-documented previously; 3) And finding a proper method to reduce shrinkage times. After understanding the possible mechanisms for shrinkage and tailoring the processing to optimize the shrinkage speed, the aim is to decrease the time for stabilization according to DIN EN 1603 from 11-18 weeks to less than 6 weeks. This would allow for reduction of storage times.

1.4 Organization of the Thesis

The work begins with an introduction of bead foams, specifically EPS as the focus, in Chapter 1, as well as outlines the project motivation and aims for research. Once the basis of the study is presented, Chapter 2 gives a detailed review of prior literature of the materials and mechanisms relevant to the study. The formation, structure, and properties of bead foams are first explained, followed by the properties and applications of EPS, pentane as its blowing agent, and its general processing. The concept of diffusivity, residual stresses, and shrinkage in EPS are also elaborated upon in this chapter, as all of these are related to the study's aim of understanding the mechanisms of EPS shrinkage behavior. Chapter 3 presents the details of the study on the dimensional stability of post-molded EPS by its three means: 1) Construction of the correlation between the volatile content in the beads and shrinkage behavior; 2) Establish a method to measure the residual stresses in foams, since this has not been well-documented previously; 3) And finding a proper method to reduce shrinkage times. The experimental methods are outlined, followed by the results and findings with respect to volatile matter content and residual stresses related to EPS shrinkage. Lastly, drawing each portion of the study together, Chapter 4 presents major conclusions of the thesis and future research possibilities based on the findings.

2 Literature Review

2.1 Bead Foams

2.1.1 Introduction

As explained in Chapter 1, bead foams are polymeric materials highly utilized in packinaging and building insulation applications. They are lightweight, low density, moisture resistant, and thermally and acoustically insulating. These materials are made of many foam particles welded together during processing, traditionally with steam. These particles as polymer microgranules impregnated with a blowing agent, expand during processing into individual beads, then undergo welding and molding into whatever shape is desired. Bead foams are unique in the sense that they combine the possibility of producing complex geometries with a low-density material, and are desirable for their good energy absorption, insulation, impact resistance, floatation, and heat resistance. They share similar properties also with extruded foams of the same density, including high energy absorption at impact, acoustic insulation, and low thermal conductivity. However, bead foams have the capability, with densities as low as 15-20 g/L, to achieve more complex geometries at with a lower weight than their extruded foam counterparts, also exhibiting higher dimensional accuracy. Thus, these materials are highly desired in industrial building insulation applications [39, 53].

2.1.2 Formation Fundamentals

Bead foams consist of two phases: a solid polymer matrix and a gaseous phase that contributes to the cell formation [39]. The bead foam creation process generally follows four steps, from homogenization of the polymer with a blowing agent, to cells nucleating in the polymer, followed by cell growth, and finally cell stabilization [53]. This schematic is illustrated in *Figure 9* at the end of Section 2.1.2.

2.1.2.1 Homogenization

Homogenization of the polymer with a blowing agent is a mass-transfer process, where the blowing agent diffuses into the melt or solid bead and stays in the polymer-gas solution [53]. The diffusion of the gas is dependent on the pressure and gas concentration in the polymer, meaning it depends on time and space; with an increase in free volume available, diffusivity increases. Henry's law describes the gas solubility in a polymer depending on pressure. Increasing the temperature leads to an exponential decrease in solubility. An increase in shear rate, however, leads to a decrease in free volume as polymer chains align, which in turn decreases the solubility [53].

2.1.2.2 Cell Nucleation

After the polymer is homogenized with the blowing agent, cells are formed from nuclei, which act as the cell centers after a pressure drop or temperature increase during processing. This sudden pressure drop or temperature increase leads to a super-saturated melt with a decreased solubility, which acts as a driving force to decrease the

gas content of the polymer-gas mixture. Cell nucleation begins at clusters of gas molecules inside the melt, according to nucleation theory, which act as nucleation sites. A high pressure drop leads to a high nucleation rate [53].

For the material, cell nucleation depends on the surface tension between the polymer melt and the gas [53]. It involves the transformation of small clusters of gas molecules into energetically stable groups or pockets. A minimum energy into the system is required to break the free energy barrier [39]. To form cells in the polymer, the free energy of the system ΔF must be increased, as described in the expression below:

$$\Delta F = \gamma \cdot A \qquad \textit{(Equation 2)}$$

Here, γ is the surface tension of the liquid and A is the total interfacial area between the gas and polymer [35].

Cell nucleation can also occur as a result of elongation or shear stress. Extensional stress around growing cells lead to pressure fluctuations, which in turn decrease the solubility. The super-saturation of the melt then increases, leading to an increase in nucleation rate and higher cell densities. Similarly, shear stresses cause micro-voids in the system. This leads to the elongation of currently-existing bubbles, which in turn increases nucleation rates and creates higher cell densities [53].

There are two types of cell nucleation in a gas-polymer system [53]. In homogenous nucleation, cells are nucleated randomly in the polymer melt matrix. It requires higher nucleation energy to begin, and nucleation occurs at certain preferred sites such as phase boundaries or additive particles. Classical nucleation theory

describes microcellular foaming during homogenous nucleation. An increase in the saturation pressure or the rate of pressure drop leads to an increase in the number of cells nucleated. When the amount of gas in the polymer increases as well, there is a higher chance to nucleate more cells. A higher pressure drop, however, requires a shorter time period. This means already-nucleated cells do not have the chance to grow very much, and thus more gas is used for cell nucleation rather than cell growth. This leads to high cell density microcellular foams [39].

During heterogeneous nucleation, on the other hand, cell nucleation is promoted at some preferred sites. Blending fillers enhance the cell population density in the foam structure. Sites in the polymer matrix with non-dissolved gas become cells. Due to surface tension, the polymer melt cannot fill some micro-pores and gaps between the two phases during mixing. Thus, space accumulates for gas, leading to cell nucleation. The process requires less gas than homogenous nucleation to make fine cells. The surface geometry of the nucleation sites depends on the nucleation agents, the presence of unknown additives or impurities, and the nature of the internal walls of the processing equipment, thus varying by site. The phase boundaries between the additive and the polymer matrix have a lower free energy barrier than in homogenous nucleation, so nucleation is more likely to occur there. The amount of additive determines the number of cells nucleated with this process. When the additive particle size is fine and well-dispersed, a uniformly-distributed microcellular structure results [39].

2.1.2.3 Cell Growth

After nucleation, cells continue to grow as the gas diffuses from the polymer matrix. A pressure drop or temperature increase during processing leads to super-saturation in the melt. In turn, the stored gas diffuses out of the melt and into the nucleation sites, causing cell to grow [39]. The growth from microgrules to foam beads is shown below in *Figure 8*. Individual spherical cells grow in the liquid polymer with the minimal surface area for a given volume in order to minimize the surface area of gas-liquid interface [44]. If the pressure inside the cells is greater than that of the surrounding melt, the cells grow to decrease the pressure difference between the inside and outside of the bubbles.

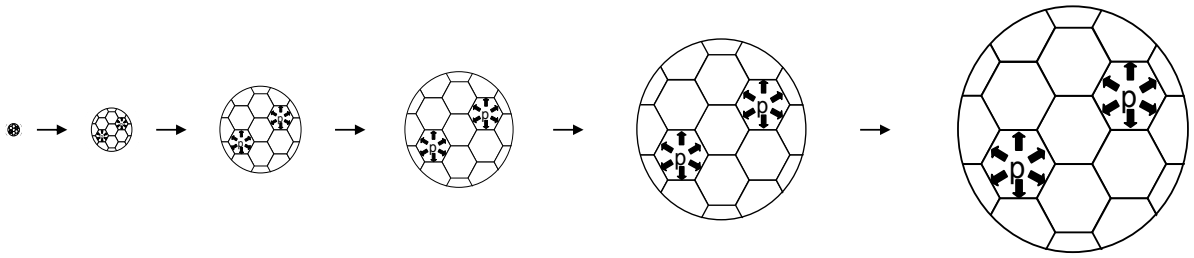

Figure 8: Expansion of EPS microgranules to pre-foam beads by cell nucleation and cell growth. [14]

Since the melt is subject to elongation deformation during cell growth, its viscoelastic properties are significant, as well as the diffusion coefficient, and diffusion kinetics through melt to bubble gas concentration, and number of nucleated cells, which are influenced by temperature [39, 44]. Additionally, nucleation times affect cell growth. When there is a sudden pressure drop during foam extrusion as the melt passes

through the die, nuclei appear at nearly the same time. Cell growth is also affected by cell coarsening. When the amount of gas diffusion between close cells is not equal, smaller cells shrink at the expense of the larger ones, leading to cell coarsening [44]. Cells coalesce because it decreases the total energy by decreasing the surface area of the cells, deteriorating the initial cell density [39]. For a given foam volume, the system is more stable with fewer large cells, which favors the combination of cell coalescence [35]. Cells also merge to coarsen when their neighboring faces fracture [44]. At equilibrium, the gas pressure in a spherical cell is larger than the pressure in the surrounding fluid, described by the expression below:

$$\Delta p = \frac{2\gamma}{r} \qquad \textit{(Equation 3)}$$

Here, r is the radius of the bubble, γ is the interfacial surface tension, and Δp is the differential pressure. The differential pressure is larger for small cells at a fixed surface tension. Small cells equalize pressures by growing faster, by breaking walls separating cells, or when the blowing agent diffuses from small to large cells. At equilibrium, the gas pressure in a small cell is larger than in a large cell, with the difference given by:

$$\Delta p_1^2 = 2\gamma \left(\frac{1}{r_1} - \frac{1}{r_2}\right) \qquad \textit{(Equation 4)}$$

Here, Δp_1^2 is the difference in pressure between two cells with radii r_1 and r_2. Gas diffuses from the smaller cells into the larger ones. Both factors favor losing small cells for the increase in size of large ones with enough time [35].

2.1.2.4 Cell Stabilization

Foams are thermodynamically unstable [35]. If cells were to continue to be allowed to grow infinitely, they would coalesce, which in turn weakens the final foam morphology [53]. Thus, cell growth must eventually be stabilized, which is promoted by a number of factors. Increasing the required surface area increases the free energy, so an activation energy is necessary for the small area increase needed for. A decrease in the surface excess of the absorbed component, which is a surface tension depressant, increases the surface tension as cells grown and thin out. Thus, the component flows from high concentration of surfaces and brings liquid polymer, leading to a self-healing effect [35]. Lastly, increasing the viscosity of the polymer phase, either by cooling or further polymerization, is the main factor of cell stabilization [35, 53]. This occurs because as the blowing agent diffuses out of the polymer, viscosity increases, since the dissolved gas in the polymer acts as a plasticizing agent. Strain hardening is induced by long chain branching, the introduction of high-aspect-ratio nano-additives, or blends with a fibril morphology. It causes thin sections of the cell walls to be subject to higher strains and a higher °ree of chain stretching, making them harder to extend than thicker portions of the cell walls. Thus, thick segments are extended more easily, leading to the "self-healing affect" of the melt [53]. Cell stabilization is a critical final step in the bead foaming process, and can affect the final foam. Too much rupture before stabilization leads to collapsing of the foam. Additionally, cooling a closed-cell foam before stabilization leads to a decrease in pressure in the cells, then causing shrinkage in the

material. Ultimate stabilization occurs because of a chemical reaction to a point of complete gelation, or cooling below the second order transition point of the material so there can be no more polymer flow [35].

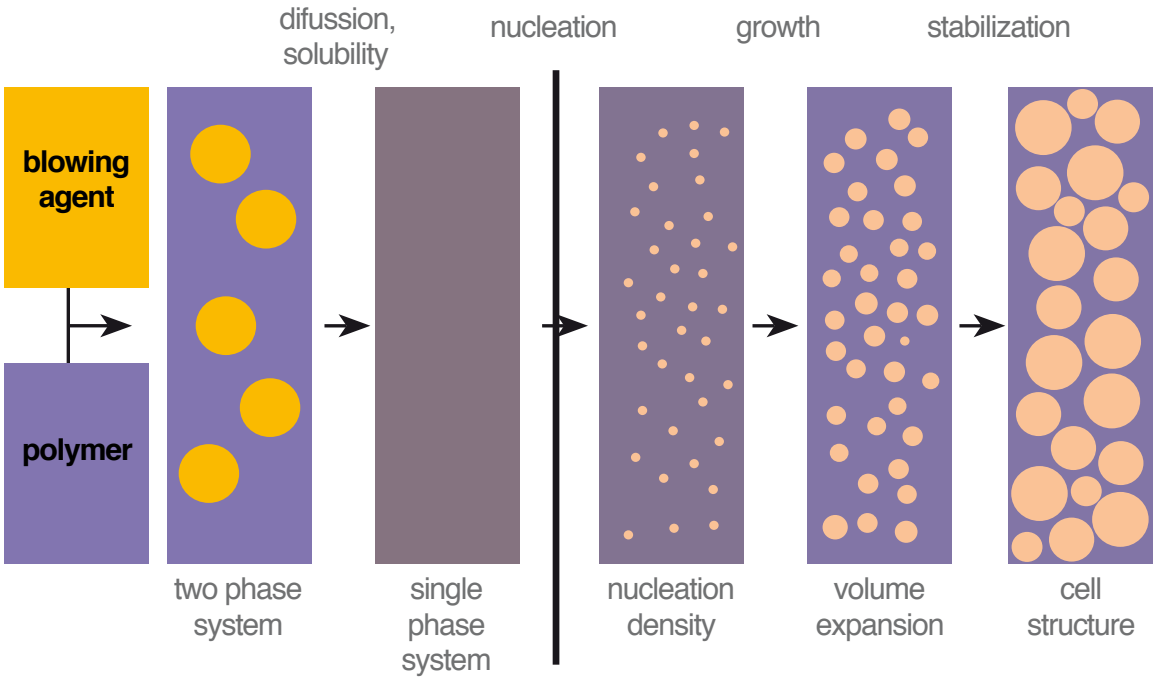

Figure 9: Pentane blowing agent and polystyrene polymer interaction during EPS cell formation. [12]

2.1.3 Bead Foam Structure and Properties

2.1.3.1 Cell Structure

Bead foams are the only foams to combine a nearly free choice of shape with a very low density below 2% of their non-foam polymer counterparts [53]. They consist of six main structural levels:

- The primary chemical structure of the polymer matrix
- A secondary structure, which is a space configuration of three-dimensional or linear cross-linked macromolecules
- The super-molecular structure consisting of cell walls
- A macro-cellular structure based on the type, number, and size of cells
- A micro-cellular structure depending on the type, number, location, and size of microcells
- A super-cellular structure, which is a distribution of macro- and micro-cells and density over the area of the foamed polymer [35]

Thermoplastic bead foams are categorized by their cell size and cell population density (conventional, fine-celled, or micro-cellular), foam density, and cell structure (open or closed cells). The foam density is dependent on the level of expansion of the original microgranules during processing. High density foams are only expanded up to four times their original size, medium density foams undergo four to ten times expansion, and low density foams have greater than ten times expanded beads. High density bead foams are generally used as construction materials, furniture, and the transportation of products, whereas low density foams are found in impact absorption, sound insulation, and packaging applications [39]. The polymer state and the cell geometry of the foam are closely related, as they are determined by forces exerted during the expansion and stabilization phases [35]. The average cell size of foams is important for air flow and process quality control in order to avoid uncontrolled face fracture which would lead to eventual foam collapse [44].

Mechanical stresses during foaming that are not uniformly distributed through the plastic foam volume lead to gas bubbles that expand along the directions of minimum local stress. The cell stretching in the foaming direction is more prominent in foams made by free-rising rather than expansion in a closed space. The lower the density, the more stretching can be observed. Certain anisotropy of the foam morphology can have a greater affect on the strength of the foam that the chemical nature of polymers, foam density, and the number of cells. Most commercial foams have anisotropic cell structures, but those foams used in structural applications exhibit isotropic structures.

Density has the greatest effect on mechanical properties of a given foam composition. It is because final density and external forces that are exerted on the cell structure before stabilization in the expanded state determine the cell shape. If there are no external forces, spherical or ellipsoidal cells result with 70-80% of the total gas volume. The higher the gas volume, the more packed and regular dodecahedron shape the cells have. The presence of external forces, on the other hand, would lead to elongated or flattened cells [35].

2.1.3.2 Open versus Closed Cells

The cell structure of bead foams can be classified into two possibilities: open cell or closed cell, differentiated below in *Figure 10*. Open cell foams have inter-connected cells through which air can freely pass [35, 39, 44]. They have higher absorptive capacity for water and moisture and higher permeability to gases and vapors. They are less effective as insulation for heat and electricity and have better sound absorption and

dampening than closed cell foams. Open cell foams are often a created with elastic polymers as the raw matrix material [35].

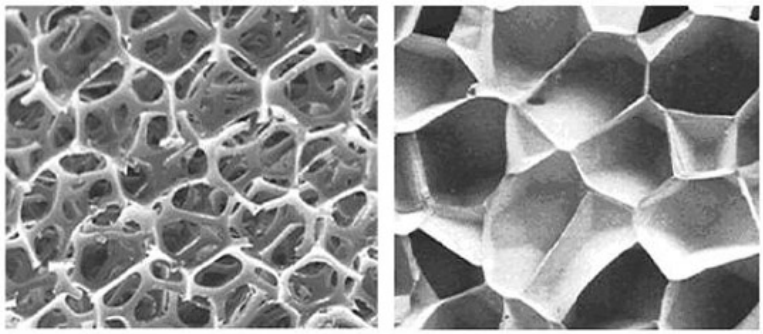

Figure 10: The two different types of possible cell structures: open cell (left) and closed cell (right). [9]

If the cell membranes around bubbles remain intact, on the other hand, closed-cell foams arise. Examples include foams made from epoxy resins, polyurethanes, silicones, and polystyrene [35]. Closed-cell foams have no openings in their cell walls. This allows for further expansion of each cell in the foamed beads during the bead foaming process without loss of expansion agents through cell wall openings [39, 44]. They have discrete walls where the gas phase of each cell is independent of that in other cells. Closed-cell foams are produced when cell membranes are strong enough to withstand rupture at the maximum foam rise and the modulus of the polymer increases quickly to a high level so the cells are dimensionally stable despite the partial vacuum development within. The isolated cells of these foams contain hydrogen, carbon dioxide, and volatile liquids that depend on the blowing agent. Over time, this matter is replaced by air from diffusion, which affects the shape stability of the foam [35]. Dry closed cell

foams generally have three faces that meet at each edge of 120° if the surface energy is minimized, and three cells and four edges that meet at each vertex. When spherical beads are steamed during molding, they expand into approximately polyhedral shape. Since they have polyhedral cells, they obey the space-filling packing rules of polyhedral. Euler's formula states that for any convex, three-dimensional polyhedron with E edges, F faces, and V vertices:

$$V - E + F = 2 \qquad \textit{(Equation 5)}$$

Bead boundaries often become fracture surfaces in closed-cell foams. Additionally, open air-filled channels can exist between three beads, which connect into a continuous network that helps with long-distance steam and gas flow during molding [44].

Even for the same density and number of open- or closed-cells, the strength and thermophysical parameters can differ for bead foams with the same polymer due to differences in cell shapes and sizes. Increasing the cell size above a certain threshold value, which is approximately 2-5 mm, leads to convective fluxes in the gas-filled cells [35]. The average cell size is important for gas flow resistance in open-cell foams, and since different cell sizes affect the shape of stress-strain curves in open-cell foams. In closed-cell foams, the mean cell size affects the gas diffusivity and thus high strain creep mechanisms, in addition to having a small influence on heat transfer [44].

2.1.3.3 Properties

Compared to their solid plastic equivalents, bead foams exhibit higher specific tensile strength, higher toughness, better thermal and sound insulation, and are much lighter [39]. Their properties depend on the composition (properties of parent polymer and gases) and geometry of the foam structure. The condition of the polymer phase, such as the orientation, crystallinity, previous thermal history, and chemical composition, determine the properties of the phase. Increasing the density increases the flexural, compression, and tensile strength and moduli. Varying the cell size and cell wall thickness, in turn, can control the density of the foam; foams of the same density have cells of different sizes. The cell size affects mechanical, optical, and thermal properties, and polymer composition, density, and cell shape affect tensile strength. Increasing the cell size makes more paths available for heat transfer by radiation or convection, which in turn increases the thermal conduction of the foam. It also increases the Young's modulus of both flexible and rigid foams, and decreases the compressive strength of foams under high compressive loads. Decreasing the cell size, however, increases the tensile strength and ultimate elongation of flexible foams [35].

In lightweight plastic foams, the cell structure fails when the ribs of the weakest transverse layer fail. Lightweight foams generally have three well-defined regions of their compressive diagrams. They begin with an initial region of sharp increase in deformation, corresponding to the compression and bending of cell ribs and walls until they buckle due to total loss of resistance, followed by a plateau region with a slight

increase in strain. During this second region, the ribs either buckle and fail leading to a sharp drop in load, or they bend due to forced elastic strain and thus lead to a minor increase in load. Lastly, there is an area of sharp decrease in resistance to deformation, defined by the final crumpling of buckled ribs and gradual compaction of the polymer [35].

The thermal conductivity of bead foams, λ, is determined as the sum of the thermal conductivities of each phase and composition:

$$\lambda = \lambda_s + \lambda_g + \lambda_c + \lambda_r \qquad \textit{(Equation 6)}$$

Here, λ_s is the thermal conductivity of the solid phase, λ_g is the thermal conductivity of the gas phase, λ_r is the radiative component, and λ_c is the convective component, which is usually ignored because most cell diameters are less than 4 mm. If the bead foam is used as an insulating material, each term contributing to the total thermal conductivity, λ, must be minimized. The solid phase contribution, λ_s is very small because the polymer thermal conductivity is intrinsically never high, and the polymer phase only makes up a small fracture of the foam volume. A further decrease in the λ_s contribution by decreasing the solid volume fraction, however, is not always possible (because it is not necessarily possible to produce a polymer at very low density), feasible (for economic and technical reasons), or desirable (because decreasing the density leads to lower strength of the foam). The gas in cells does most of the heat transfer, as the foam is over 90% gas by volume. However, since many blowing agents are available depending on the specific bead foam and application, λ_g varies. The

radiative contribution to heat exchange depends on the radiative capacity of the starting polymer material, and is also influenced by the temperature gradient between the sample surfaces according to the Stefan-Boltzmann law. The proportion of total heat exchange because of radiative heat transfer depends on cell size and wall transparencies. Radiative heat transfer occurs through the wall separating any two cells in a particular orientation. Thus, a foam with a large amount of small cells has less radiative heat transfer than one with few larger cells. This means that increasing cell size affects the overall thermal conductivity more than increasing the density. Since most commercially-produced foams have smaller cell sizes, the convective heat exchange contribution to total heat transfer is very small, only detectable in very lightweight foams. Ultimately, the different mechanisms of heat conductivity in bead foams depend on the cell size. Low density and small solid polymer content foams have large cell size and thus favorable conditions for heat transfer. High density means a greater number and thickness of cell walls, which leads to increased heat insulating screens between cells and thus a smaller radiative component [35].

2.1.4 Blowing Agents

2.1.4.1 Introduction

Bead foams contain blowing agents, which serve as the means of expansion from their original, compact microgranules to light, cellular foams. The impregnation of bead foams with their blowing agent involves saturating the solid polymer beads with a

gas close to the polymer's melting temperature, then releasing the material full of blowing agent into an expansion vessel. The beads are then washed to remove any residual suspension stabilizer, which would inhibit proper bead welding later in the processing [53]. A homogenous polymer and blowing agent solution is crucial for the final cell morphology and mechanical properties of the material [39].

The amount of blowing agent injected into the polymer is a significant factor in the final product. It must be below the solubility limit of the processing pressure and temperature to allow for complete mixing and dissolving of the gas into the polymer. If excess blowing agent cannot be dissolved into the polymer, large voids form in the foam. Thus, the solubility of the blowing agent that can be absorbed or dissolved into the polymer at different temperatures and pressures must be determined. The maximum solubility of gas into a polymer varies by system, and is described by Henry's law:

$$c_s = Hp_s \qquad \textit{(Equation 7)}$$

Here, c_s is the solubility of gas in the polymer (cm^3/g or $g_{gas}/g_{polymer}$), p_s is the saturation pressure (Pa), and H is Henry's law constant (cm^3 [STP]/g-Pa), defined as:

$$H = H_0 \exp\left(-\frac{\Delta H_s}{RT}\right) \qquad \textit{(Equation 8)}$$

Here, H_0 is the solubility coefficient constant (cm^3 [STP]/g-Pa), ΔH_s is the molar heat of sorption (J), R is the gas constant (J/K), and T is the temperature (K). When a blowing agent dissolves in a polymer, the weight of the impregnated blowing agent increases

the polymer's molecular weight. Thus, weighing the polymer in a pressurized gas gives the solubility and diffusion coefficient of the gas [39].

As a good blowing agent is crucial for proper material mechanical and heat-insulation properties, a number of traits are sought after when choosing a blowing agent for a system [30]. It is primarily desirable to have high solubility at high processing temperatures and low solubility at ambient temperatures, as this improves the processibility because of a lower system pressure, better mixing, better size control, and less plasticization of cellular polymers. As further features, ideal blowing agents should have low toxicity, low ozone depletion potential, low global warming potential, low flammability, and be low cost [35].

2.1.4.2 Chemical versus Physical Blowing Agents

Blowing agents are classified as chemical if they are compounds that undergo a chemical transformation during the foaming process, or physical if they are not subject to chemical transformation and rather are gases used for foaming [35]. Chemical blowing agents decompose at certain processing temperatures and evolve gases such as carbon dioxide and nitrogen. They can in turn be divided into two groups based on the enthalpy of reaction being exothermic and thus releasing energy during the gas generation reaction, or being endothermic and absorbing energy during this process [39].

Physical blowing agents, on the other hand, are injected into the polymer system as a liquid or gas, some of which, such as pentane, have a low boiling point and thus stay in liquid state in the polymer under the melt pressure. When pressure is released, the blowing agent changes immediately to a vapor, which comes out of the solution with the polymer and thus expands the polymer melt [39]. Physical blowing agents ideally should have the following characteristics:

- An inert liquid phase so they don't affect the chemical and physical properties of other components or the polymer
- Sufficiently soluble in or mix readily with foaming formulation
- Have a gaseous form that is thermally stable and chemically inert
- Have low vapor pressure at room temperature to facilitate storage
- Be highly volatile under external heat or reaction heat, and have low heat capacity and low latent heat of vaporization
- In gaseous form, hey should have a lower rate of diffusion in the polymer than air to migrate shrinkage
- Be properly compatible with materials
- Not be highly flammable or combustible
- Nontoxic, odorless, economically feasible, and environmentally safe

Common blowing agents include low-boiling, volatile liquids, such as aliphatic and halogenated hydrocarbons such as chlorofluorocarbons and hydrofluorocarbons, low-boiling alcohols, ethers, ketones, aromatic hydrocarbons, and solid adsorbents

saturated with gases or low-boiling liquids [35, 39]. The most frequently used blowing agents in industry include fluorocarbons, chlorofluorocarbons, pentane, and butane. Due to their high solubility, these blowing agents can be dissolved in large quantities into polymer matrices. This allows for a foam structure with a high void fracture at low processing pressure and large volume expansion because of the small amount of gas loss. A large blowing agent molecule size, additionally, leads to low diffusivities and thus less gas lost out of the foamed extrudate and a low foam density in the final product [39].

2.2 Expanded Polystyrene (EPS) Foam

2.2.1 Polystyrene

Polystyrene is a clear, brittle, versatile thermoplastic resin [35]. It is found naturally in plants and different foods such as fruits, vegetables, and nuts, and is also produced at the industrial level from ethyl benzene [13]. Polystyrene is used in a variety of applications due to its properties. With an annual consumption of 11.5 million tons in 2004, it is one of the most quantitatively significant chemicals [41].

At temperatures below its glass transition temperature (T_g) of 100 °C, polystyrene is a solid, glassy polymer. Above its T_g, the polymer is malleable and rubbery with viscous liquid properties, making it possible to process [19, 41].

EPS bead foam is made from expandable polystyrene beads, which are rigid cellular plastics containing pentane as a blowing agent. Since pentane is contained in

petroleum and styrene is a petroleum derivative, both substances are pure hydrocarbons, and thus EPS is made up of only carbon and hydrogen [13].

2.2.2 Properties and Applications

2.2.2.1 Advantages and Disadvantages

EPS is the most widely used bead foam material because of its low price and high availability [53]. Its low density, thermal and acoustic insulation capabilities, as well as consistent performance make it commonly used in insulation and packaging applications [39, 53]. The low density also gives EPS low strength and stiffness properties. This makes EPS idea for cushioning applications (because of its low stiffness), energy absorption (because of its low strength and large compression), and thermal insulation (because of its low thermal conductivity) [35]. Compared to EPP foam, EPS has a worse compressive set and is therefore less used in applications with multiple impact deformation. However, since EPS microgranules are able to retain the blowing agent within, transportation of the material is much cheaper than EPP, since EPP must be transported as foamed beads which occupy more space than EPS microgranules [53].

2.2.2.2 Mechanical Properties

The mechanical properties of EPS depend on the density of the foam and welding quality of the beads, and involve three interacting levels: the polymer microstructure that affects the mechanical response, the cell edges and faces, as well

as the cell geometry [13, 35, 44]. The polymer contribution of the foam, however, dominates the mechanical properties [44]. The mechanical strength of EPS when it undergoes short-term and sustained loading is significant; the compressive stress values correspond to less than 2% of the compressive strain [13]. As foam, EPS is softer than its solid counterpart, thus Young's modulus is measured in compression rather than in bending or shear. Increasing the material's temperature at a constant rate leads to temperature dependence of the elastic moduli [44]. At low densities, the tensile modulus is approximately linearly related to the density of EPS, but it increase at high densities with high power of density. Increasing the density as well as the cell size also leads to a linear increase in tearing energy [35].

2.2.2.3 Thermal Properties

98% of EPS is air, thus making the foam a good thermal insulator with so much air trapped within the cells. Additionally, since air stays within the cells, the insulation also remains constant [13]. Convection is neglected, as most cells are less than 3 mm in diameter, but conduction occurs through the solid cell walls as well as the gas within cells. The polymeric matrix conduction is affected by the crystallinity and orientation, which in turn are affected by the foaming process. For low densities, the cell gas conduction dominates the thermal transport over the solid polymer due to its high volume fraction. For very small cells, cell gas thermal conductivity decreases. Radiation of EPS is dependent on cell morphology and temperature. Adding graphite decreases the thermal radiation, which in turn decreases overall conductivity, as the graphite

particles are reflectors for infrared radiation [53]. The thermal conductivity is density-dependent; at 10 °C for EPS foam with density 20 kg/m^3, it is between 0.035-0.037 W/(m·K) [13]. As the specific heat of cellular polymers is the sum of the specific heats of each component, the contribution from the gas is neglected because it is so small [35].

2.2.2.4 Other Properties

EPS is a non-hygroscopic material, meaning it does not keep any water molecules it may absorb. Because of its waterproof cell walls, water can only penetrate the foam through any possible inter-bead channels. Thus, the amount of water the final product takes in depends on how the raw material behaves when it is processed, as well as upon the processing conditions, but is independent of density [13]. Its ability to resist °radation from water absorption makes it attractive in its numerous packaging and insulation applications [24].

Compared to basic polystyrene products, EPS is less resistant to chemicals. Its cell structure allows for a higher surface area of material, and thus quicker and more damage form chemicals, especially for low-density products. It is, however, very resistant to aging, and undergoes no rotting over time [13].

2.2.2.5 Applications

With a makeup of 98% air and low density, EPS offers excellent thermal insulation, and is cost-effective with a better price/performance ratio and lifetime durability compared to other insulation products [24, 39, 53]. Thermal insulation is the

largest application for rigid cellular foams because of the thermal conductivity, application ease, cost, moisture absorption, and water vapor transmission of the materials. Their use in construction for wall and ceiling insulation for residential buildlings has increased over 200% in the past decade [35]. Additionally, with such high air content, its lightweight nature saves fuel and transportation costs significantly [53]. It is also used to ensure safety from transportation damage as energy absorbers or spacers in packaging [39, 53]. It is attractive for packaging applications due to its low cost, ease of application and fabrication, moisture susceptibility, thermal conductivity, and mechanical properties [35]. Its ability to absorb both impact sound in floating floors and airborne sound for walls makes it desirable as acoustic insulation. Because EPS does not retain or degrade from absorbed water, its moisture resistance also makes it applicable as packaging or cooling material for perishable goods [24, 39, 53]. Additionally, the production process is highly flexible, making the material's mechanical properties adjustable to fit more applications. The manufacturability of EPS into many size and shape molds combined with its compatibility with a variety of materials makes it also very versatile [53].

2.2.3 Pentane Blowing Agent

Amorphous thermoplastic resins like polystyrene only retain blowing agents in their solid state, i.e. at temperatures below T_g. Impregnated polystyrene granules containing trapped blowing agent within are expanded before the welding process during the pre-expansion stage of processing. This allows for efficient transportation of

the un-foamed blowing agent impregnated polymer, as well as density control by the manufacturer who is making the EPS foam itself. The expandable polystyrene beads are made by suspension-polymerization with the pentane blowing agent. Granules are first formed during polymerization, then the pentane is added and diffusion occurs into the granules [53]. As a low-boiling liquid, pentane is dissolved into the polymer and then converted to gas by heating or decreasing the pressure [35]. The pentane acts as a polymer plasticizer [30].

Increasing the amount of blowing agent in EPS leads to greater expandability. However, too much blowing agent leads to rapid permeation, and can cause both shrinkage collapse and heat sensitivity of the foam. Additionally, increasing the amount of time that the blowing agent remains in the EPS beads increases expandability and decreases shrinkage rate [31].

2.2.4 Processing – General

2.2.4.1 Microgranule Formation

EPS is made from pentane-impregnated polystyrene microgranules which are later expanded during processing. To make the initial microgranules, pentane is introduced to suspension-polymerized polystyrene, and the polystyrene beads are left to absorb up to 8 wt% of the pentane. Since pentane is a plasticizer, it decreases the polymer's glass transition temperature from 100 °C to about 60 °C, depending on the amount. Microvoids formed inside the beads serve as sites for cell expansion later [44].

Figures 8 and 9 in Section 2.1.2 shows the changes in the foam with respect to the blowing agent during the course of the processing lifetime. These microgranules with pentane within are then transported as EPS raw material.

2.2.4.2 Pre-Expansion

Once received by EPS producers, the microgranules undergo the first step of processing as per *Figure 11* below, pre-expansion, where they are expanded at 100-110 °C with input steam [13]. This temperature is chosen because heating to less than 100 °C results in a stiff polymer and thus sluggish expansion, 110-120 °C causes bead sensitivity to shrinkage and heat, and over 120 °C softens the polymer too much, thus leading to too rapid of a loss of blowing agent [31].

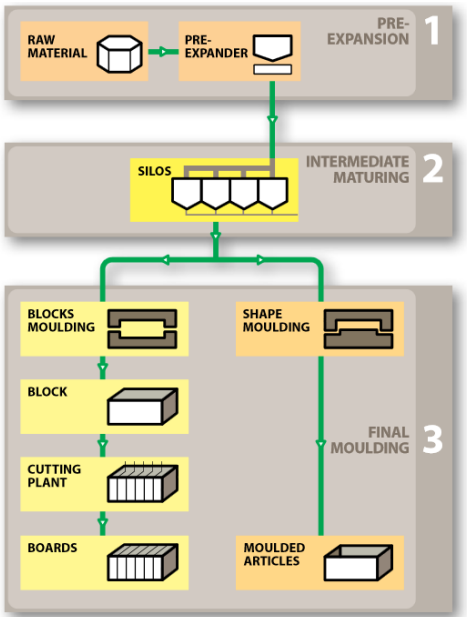

Figure 11: EPS processing lifetime, from raw material to final product, in 3 main steps. [24]

The high temperature softens the beads and the blowing agent inside expands the beads 40-60 times their original size [13]. During this step, the density falls from approximately 630 kg/m^3 to between 10-35 kg/m^3 [24]. The final bulk density, which determines the foam density, depends on the temperature and steaming time [13]. The primary expansion step is controlled by temperature and time. Increasing the temperature leads to a softer polymer, a higher expansion rate which thus leads to uneven expansion because of inconsistent pentane content, bead size, or cell structure, and an increased permeation rate of the blowing agent [31]. During the expansion step, the microstructure also changes. Microvoids that formed earlier expand into near-spherical voids. The compact microgranule beads turn into cellular, plastic beads with small closed-cells that hold air in the interior, illustrated below in *Figure 12* [24, 44].

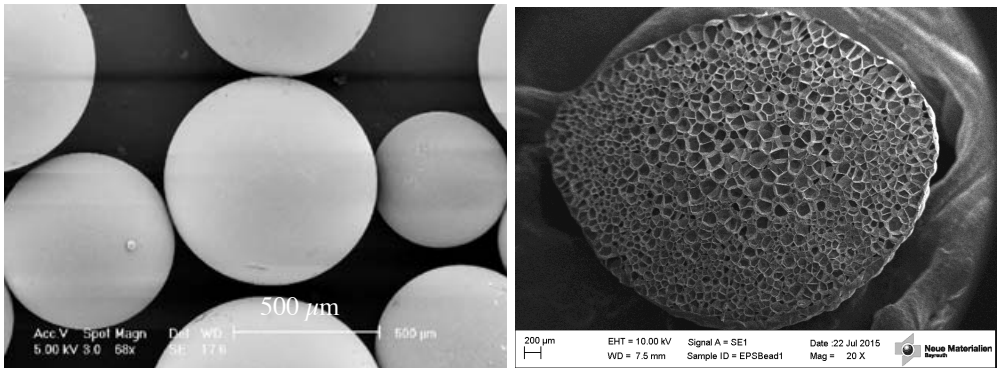

Figure 12: Microstructure changes that take place during EPS processing from microgranules (left) to pre-foamed beads (right). [65, Author]

Pentane within the EPS beads breaks down into CO_2 and water in the earth's atmosphere during the pre-expansion step [13]. As the polystyrene beads are heated,

the pentane evaporates at approximately 50 °C. Longer heating times lead to cell collapsing, since pentane escapes faster than air diffuses into the cells [44]. Cell growth is dependent on the pressure difference between the inside cell and the surrounding medium. Decreasing the external pressure or increasing the internal cell pressure leads to a greater pressure difference [35].

2.2.4.3 Intermediate Ageing

After leaving the pre-expander, the EPS beads are left to cool and stabilize in silos for approximately 12-48 hours so that the pressure between the internal cells and the atmosphere equilibrates [13, 39]. The residual blowing agent condenses and desorbs, causing a partial vacuum within individual cells, shown below in *Figure 13*; this pressure is equalized by storing the beads to allow air to diffuse slowly into the beads [13, 30, 31].

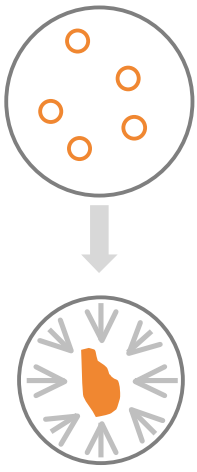

Figure 13: Schematic representation of residual blowing agent condensation in EPS foam cells after de-molding, causing an internal vaccum and thus shrinkage. [Author]

Decreasing the blowing agent level is key during the ageing step, as too high blowing agent levels can lead to excessive cooling times and high molding sensitivity. The beads are susceptible to collapse from thermal shock or over-expansion, crushing because of the internal vacuum, or shrinkage due to rapid blowing agent loss [31]. Cooling is affected by vaporization of the blowing agent, gas expansion, and heat loss to the environment [35]. This ageing step allows the beads to have better mechanical elasticity and expansion capacity, as an internal vacuum makes the beads susceptible to deformation [13, 31].

2.2.4.4 Steam-chest Molding

During the final EPS processing step, pre-expanded foam beads are welded together with steam-chest molding. Steam passes through a metal mold with the beads at a pressure of approximately 1.29-1.98 bar, which corresponds to a temperature of 107-120° C, above the T_g of the polystyrene with pentane [13, 44]. The high pressure steam softens bead surfaces, causing inter-diffusion of polymer chains between different beads and thus bead cohesion. Better inter-bead cohesion and fewer macro-voids result in better mechanical properties of the foam [53].

The five basic steps of steam-chest molding process are illustrated in *Figure 14*. During the steam-chest molding process, polymer chains diffuse across inter-bead regions during heating. The final cooling freezes the physical entanglement of the polymer chains at the inter-bead boundaries, leading to bonding. In the mold-filling

second step, the pre-expanded beads are drawn by air pressure into the mold by an injector according to the Venturi principle. This step is critical for homogeneous bead distribution inside the mold. The steaming third step is crucial for good welding; high temperature, sufficient steam time, and high contact area and force between beads are desired. During the final two steps, the mold is sprayed with water until it reaches a cooled temperature of approximately 80° C. This step is critical, as ejection without cooling means further bead expansion and thus deviation from the originally intended size [53].

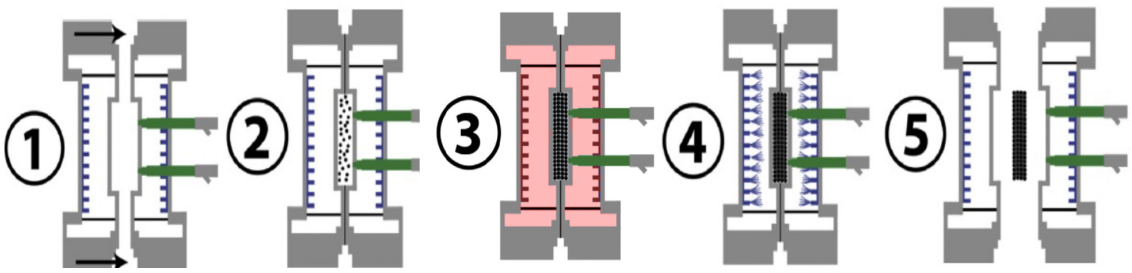

Figure 14: Steam-chest molding processing steps, showing 1) closing of the mold, 2) filling of the mold, 3) steaming, 4) stabilizing by pressure controls, and 5) ejection of the part. [Re-made from 53]

2.3 Diffusivity

Gas diffusion in closed-cell polymeric foams is more complicated than through solid polymer films because of the additional variables of cell size, wall thickness, density, and porosity. It is related to diffusivity of the polymer and foam structure [44]. Penetrants with very small molecules have concentration-independent diffusion coefficients; large organic molecules, however, have concentration-dependent diffusivity

[39]. Foam is a multi-layer laminate of thin polymer films and thick gas layers [29]. The pentane blowing agent must dissolve on one side of the polymer film, diffuse through the film, constrained by the solubility limit, and then diffuse through the polymer by molecule diffusion. It detaches from the other side of the membrane, transports through the gas layer by conduction or convection, diffuses out of the cells, and repeats this process until it moves out of the entire foam [29, 34]. This schematic is illustrated in *Figure 15*.

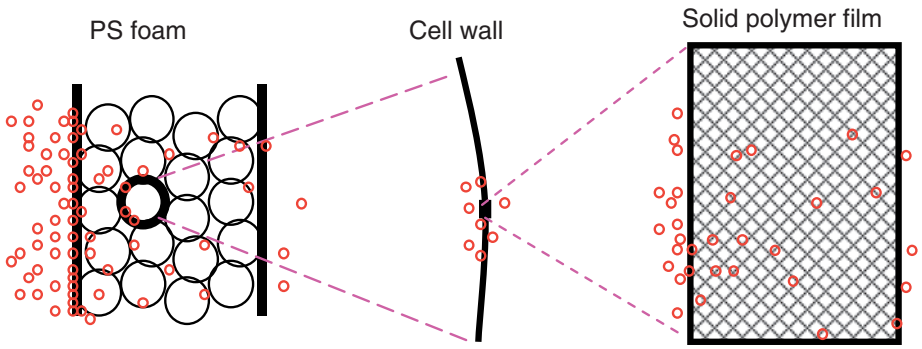

Figure 15: Hierarchical illustration of gas molecules (red) diffusion across EPS foam (black). [34]

If beads are poorly welded during processing, additional pathways for the gas to exit the foam can be formed, thus increasing the effective diffusion rates [34]. These pathways, as introduced by Kannan et al. in 2010, are illustrated in *Figure 16*:

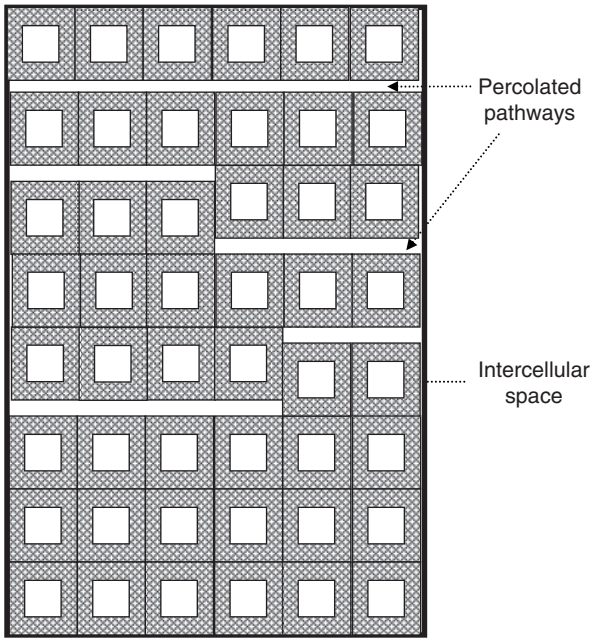

Figure 16: Inter-cellular space between individual cells in molded EPS foam, which can lead to faster diffusion by more pathways for gas to exit. [34]

The gas diffusivity of closed-cell foams is important because it affects creep and thermal conductivity, since the blowing agent can have lower conductivity than air [44]. Polystyrene has high melt strength in a wide temperature range, and low diffusivity of the blowing agent. This low gas diffusivity is favorable for keeping the blowing agent in the beads for a long time and thus being able to transport the impregnated microgranules with pentane [39]. However, the amount of residual pentane in EPS affects the strength and dimensional stability of the final material [29].

During steam-chest molding, steaming causes the bead surfaces to soften, which in turn causes wetting and van der Waals forces then dominate the cell welding

process. After, healing occurs by inter-diffusion of the polymer chains across beads surfaces, shows in *Figure 17* [53].

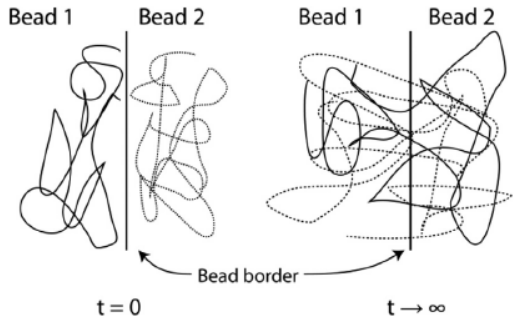

Figure 17: Arrangement of molecules in EPS before (left) and after (right) processing. There is a clear divide between beads prior to molding, which disappears as polymer chains across bead interfaces weld and form solid bonds. [53]

Polymer inter-diffusion across interfaces depends on the molecular weight, chain end distribution, and temperature history. [53]. Cell faces act as barriers to gas flow; diffusion occurs quickly across cells, and then slows down at the faces. The cells within the EPS beads act as constant pressure reservoirs with pressure gradients across the cell faces, with gas seeking the easiest route through the cell face network [44].

Fick's law, Case II behavior, or free volume theory is often used to describe blowing agent gas diffusion in EPS polymer. Fickian diffusion describes small molecules diffusing in a homogeneous matrix without entanglements, like so:

$$\frac{\delta C}{\delta t} = \frac{\delta}{\delta x}\left(D\frac{\delta C}{\delta x}\right) \qquad \textit{(Equation 9)}$$

Here, $C(x,t)$ is the concentration of the gas in position x apart from the centerline of the sample at time t, and $D(c,t)$ is the concentration-dependent diffusivity. With symmetric samples, the following initial boundary conditions can also be assumed:

$$\left.\begin{array}{l} C(x,t=0) = C_m \\ \left.\frac{\partial C}{\partial x}\right|_{x=0,t} = 0 \\ C(x=L,t) = C_0 \end{array}\right\} \quad \textit{(Equation 10)}$$

Here, C_m and C_0 are the initial and saturation concentration [39, 53]. With Case II diffusion, however, small molecules diffuse or dissolve in a network of entangled chains. This, in turn, causes swelling and thus increases the entanglement density, changing the polymer relaxation mechanism [53]. The free volume theory assumes competition between penetrants for unrelaxed free volume can lead to differences in mass transport in gaseous mixture systems [34]. The free volume within the polymer has three components: the macromolecular occupied volume; the interstitial free volume, which is small and uniformly distributed in the material; and the cell free volume, which is excess free volume large enough for gas transport, and is especially significant for glassy polymers with chains not in equilibrium [19]. The temperature dependence of gas diffusivity in a polymer is described with an Arrhenius type equation:

$$D = D_0 \exp\left(-\frac{E_d}{RT}\right) \quad \textit{(Equation 11)}$$

Here, D_0 is the diffusivity coefficient constant, R is the gas constant, T is temperature, and E_d is the activation energy for diffusion. The rate of diffusion can be increased by processing the polymer and gas mixture at a higher temperature [19, 39].

After molding, approximately 40% of the original blowing agent content of pentane remains in EPS. This residual pentane plasticizes the foam, decreasing its tensile strength and maximum usable temperature. As the foam ages, the pentane diffuses out, and EPS becomes stronger and smaller, with a higher temperature capability [29]. The diffusion rate is generally high the first couple of days, then decreases. EPS normally contains approximately 2 wt% pentane three months after de-molding [39].

2.4 Residual Stress and Creep

2.4.1 Strength of Thermoplastics

Rigid cellular polymers such as EPS do not usually have a definite yield point in their stress-strain behavior; rather, they undergo increased deviation from Hooke's law with increasing compressive load. The plastic phase composition, density, cell structure, and plastic state are all structural variables that affect the compressive strength and modulus. The cell shape and geometry of thermoplastic bead foams affect the compressive properties. The cell structure is thus often controlled during processing to optimize certain physical properties.

$$strength\ or\ modulus = A\varrho^{a} \qquad \textit{(Equation 12)}$$

Here, ϱ is the representative foam density, and A, a are constants. Decreasing the temperature increases the strength and modulus [35].

EPS foam contains inter-bead channels that are nearly isotropic. Thus the rate of creep, or change in dimensions caused by constant stress, accelerates quickly [35, 44]. Short-term creep exists in foams at all stress levels, but long-term creep only results after a certain threshold stress level [35]. When creep stresses in closed-cell foams are not enough to cause yield, they have low creep strain and no geometric nonlinearity [44]. Thermoplastic injection moldings contain residual stresses because of cooling rates through the thickness of the mold [42]. The time available for fusion of bead surfaces is approximately 10-100 seconds, depending on the mold. Thus, rapid cooling of the mold causes the outer, surface layers to solidify before the inner portions [42, 44]. The core then shrinks with more cooling because of the thermal contraction, but this shrinkage is constrained by the solid outer region which is already cooled, resulting in tension residual stresses in the core balanced by compressive stresses in the other region. These stresses decrease life expectancy of the foam, increases likelihood of dimensional instability, and lead to environmental stress cracking [42].

2.4.2 Stress-strain Responses

Various bead foams exhibit different stress-strain responses depending on their processing and shape. Polymers are assumed to be either linearly elastic and isotropic with Young's modulus, E, and Poisson's ratio ν, or to be elastic-plastic with a yield stress that increases with strain. At less than a few percent strain, the foam is idealized

as linearly elastic and isotropic. The linear elastic relationship between tensile and compressive stress and the corresponding strain is related linearly by a constant, E:

$$\sigma_x = E\varepsilon_x \qquad \textit{(Equation 13)}$$

In tensile and compressive tests, strains in other directions are related by Poisson's ratio, ν:

$$\varepsilon_y = \varepsilon_z = -\nu\varepsilon_x \qquad \textit{(Equation 14)}$$

The linear elastic model is used to describe materials with small strains, stress proportional to strain, no dependence on loading or strain rate, and materials that return to their original shape when the loads are removed with an unloading path which is the same as the loading path [44].

When the applied stress exceeds the limit of the yield stress, some strain remains permanently after the stress is removed. This behavior is less ideal for polymers than metals in general, because the slowness of the viscoelastic recovery can make the strains seem permanent. Therefore, the foam exhibits and elastic-plastic response. EPS has compressive yield stress and residual compressive strain on unloading. As a closed-cell foam, it also hardens (yield stress increases with increasing strain) because of gas compression within the cells [44].

At strains below 5%, polymer viscoelasticity dominates the compressive creep response of closed-cell foams, and at high strains cell gas dominates. Glassy polymers

such as polystyrene have much lower gas diffusivities than semi-crystallines. Thus, the gas contributes less to high strain creep [44].

2.4.3 Origins of Residual Stresses

Residual stresses are stresses that remain in a body that is no longer being subjected to external forces [70]. They arise during most manufacturing processes with material deformation, heat treatment, machining, or processing operations which somehow change the shape or properties of the material [33, 70]. In a freestanding body, there must be stress equilibrium, meaning the tensile residual stresses must be balanced by compressive residual stresses elsewhere in the body. Surface tensile residual stresses are undesirable; they lead to fatigue failure, quench cracking, and stress-corrosion cracking. Surface compressive residual stresses, on the other hand, increase fatigue strength, resistance to stress-corrosion cracking, and bend strength [33].

Residual stresses can be classified based on their origin. Mechanical residual stresses are often a result of manufacturing processes that produce non-uniform plastic deformation, and chemical ones are caused by volume changes associated with chemical reactions or phase transformations [33]. Shear residual stresses result from non-isothermal polymer melt flow into the mold, and entropy stresses from non-equilibrium molecular polymer chain orientation [66]. Inhomogeneous heating or cooling operations, on the other hand, cause thermal residual stresses [33, 66]. They lead to several thermal gradients and thus large internal stresses when coupled with material

constraints in the bulk of large components, as so occurs when EPS foam is cooled after processing, illustrated in *Figure 7* from Chapter 1 [33].

They are also classified by their size, with respect to the body. Type I are macro residual stresses, which vary within a body over a range much larger than the grain size. Type II are micro residual stresses, which occur due to differences in microstructure of the material at the grain size level such as different phases or constituents. These can be expected to exist in single-phase materials because of the anisotropy in each grain, as well as in multi-phase materials because they contain different proportions of different phases. Lastly, Type III are micro residual stresses at the atomic level, and occur for similar reason as Type II, but additionally because of dislocations or other crystalline defects [33].

2.5 EPS Shrinkage

During this post-processed period, EPS is known to undergo shrinkage that affects its ability to be used until it is stabilized. The shrinkage is affected by diffusion of the gases from the cells to the inter-bead channels and thus to the external atmosphere [44].

EPS undergoes two known types of shrinkage after de-molding: molding shrinkage and after-shrinkage, defined in Section 1.3. When a partial vacuum develops inside foams cells because the structure is not strong enough to resist the excess pressure of atmosphere over that within the cells, after-shrinkage occurs. This

shrinkage is especially difficult to overcome in low-density, flexible, and semi-flexible closed-cell foams [35]. The focus on this study is understanding this after-shrinkage in EPS foam, as it takes a long amount of time and hence leads to very high storage costs of the foam molded parts after processing.

After the EPS foam production process is complete, the blowing agent within is replaced with air by diffusion until equilibrium is reached, based on five main factors. The chemical nature of the polymer and gas, especially the permeability of the polymer cell walls to the given gas, the ambient temperature and humidity conditions during storage, as well as the fraction of closed cells and whether or not there is a compacted skin layer, are primarily significant. Additionally, cell size affects the foam's ability to reach equilibrium, as a large number of small cells resist gas exchange better than a few large cells. The foam article shape itself also plays a role. As gas is replaced by the surrounding air first in the surface portions of the specimens and then in deeper zones, thicker articles take longer to reach equilibrium [35].

Assuming polystyrene behaves viscoelastically, decreasing the intracellular pressure and temperature to room temperature and pressure leads to EPS shrinkage. After de-molding, each cell's inside is overly-pressurized relative to the ambient environment until it reaches atmospheric conditions, illustrated in *Figure 13* in Section 2.2.4.3 [27].

The amount of time needed to age EPS foam so that the shrinkage is stabilized is controlled by various factors. Increasing the density of the material, the blowing agent

molecular complexity, as well as the polymer molecular weight increases the time. Decreasing the bead size, however, decreases the time required for aging. The storage environment also plays a key role. Decreasing the airflow or increasing the ambient temperature decreases the time [31].

3 Dimensional Stability of Post-molded EPS

3.1 Introduction

After the explanation of bead foam materials an EPS, as well as outlining the motivation for this study, this chapter presents the experimental work done in this study. With the aim of understanding the shrinkage behavior of EPS foam after processing, *Table 2* below outlines the testing methods used as well as their functions.

Table 2: Overview of the testing methods for each function of interest in this thesis. *[Author]*

Function	**Method**
Crystallinity & glass transition temperature	Differential scanning calorimetry (DSC)
Volatile matter content	Thermogravimetric analysis (TGA)
Volatile matter composition	Gas chromatography with mass spectrometry (GC-MS)
Residual stresses	Hole drilling method & Raman spectroscopy
Dimensional shrinkage	Length measurements
Microstructure	Scanning electron microscopy (SEM)

3.2 Experimental Methods

3.2.1 Materials and Preparation

All experiments were performed with one type of EPS material, BASF 300E Peripor, which is a common material used as building insulation, in order to eliminate influence of material difference. The raw material was received from BASF as microgranules, then pre-expanded and molded into plates using steam-chest molding. Two different batches of 300E Peripor microgranules were used. One batch, referred to as “new,” came from a previously un-opened, sealed BASF container. These microgranules were measured with thermogravimetric analysis (TGA) to have 4.61 wt% volatile matter. The other batch, referred to as “old,” came from a prior opened BASF container. These microgranules were measured with TGA to have 4.08 wt% volatile matter. The differences in the two groups are outlined in *Table 3*.

Table 3: Two types of BASF 300E Peripor raw material microgranules used in this study. Volatile matter content was measured with TGA. The destination describes the final sample groups that were created by each set of raw material, further explained in Section 3.2.2. [Author]

Raw Material Batches				
	Material	**Origin**	**Initial Volatile Matter (wt%)**	**Destination**
"New"	BASF 300E Peripor	prior unopened, sealed BASF container	4.61	Groups 1A & 2
"Old"	BASF 300E Peripor	prior opened BASF container	4.08	Group 1B

During pre-foaming, the Kurtz X-Line 3.0 machine was pre-pressurized at 740 mbar for 11 seconds before the microgranules were pressurized at 240 mbar until the desired amount was reached. Temperature changes were controlled by pressure in order to achieve greater accuracy. The “new” group of microgranules were steamed for 48 seconds to reach a pre-foam density of 23 g/L, whereas the “old” group of microgranules was steamed for 90 seconds to reach the same density, since they contained less blowing agent (shown by their lower starting weight percent of volatile matter) and thus needed a longer amount of time to effectively expand the microgranules into foam particles. The pre-foamed material was then stored for 48

hours to allow for equilibration of the pressure between the internal cells and the atmosphere. This ageing step allows the beads to eventually create foam with better mechanical elasticity and expansion capacity [13, 31, 39]. After storage, the pre-foamed was molded into plates of size DIN A4 with a thickness of 22 mm using a Teubert TVZ 162 steam-chest molding machine. *Figure 18* below simplifies the size and shape of samples produced.

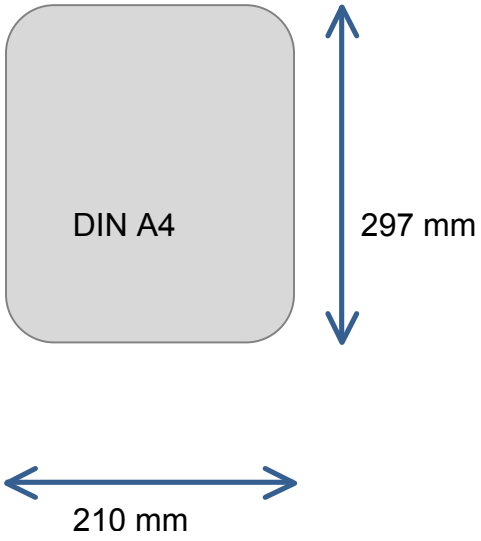

Figure 18: Size and shape of EPS foam samples used in this study. [Author]

3.2.2 Sample Organization

Samples were split into three different groups for the purpose of this study based on the origin of their raw material microgranules (described in *Table 3* from Section 3.1.1) as well as their storage conditions after molding. The first split was based on the temperature of storage after processing, summarized below in Table 3. Group 1

samples were stored in a climate-controlled cellar at standard room temperature and pressure. Group 2 samples were stored in an air-circulated oven at an elevated temperature of 60° C. The samples in Group 1 were also further split based on the microgranules from which they were made. Group 1A as well as Group 2 samples were made from the previously described “new” microgranules (refer to *Table 3*). Measured with TGA, these microgranules contained 4.61 wt% volatiles. Group 1B samples, however, were made with the “old” batch of microgranules (refer to *Table 3*). These Group 1B microgranules were measured to have an initial volatiles content of 4.08 wt%.

Table 4: Separation of samples used in this study into three groups based on raw material (microgranule) origin and storage conditions (temperature). The definition of "New" and "Old" microgranules is defined in Table 3. [Author]

Sample Grouping			
	Group 1A	**Group 1B**	**Group 2**
Material	BASF 300E Peripor	BASF 300E Peripor	BASF 300E Peripor
Microgranules	"New"	"Old"	"New"
Origin	prior unopened, sealed BASF container	prior opened BASF container	prior unopened, sealed BASF container
Initial Volatile Matter (wt%)	4.61	4.08	4.61
Storage Location	Climate-controlled cellar	Climate-controlled cellar	Air-circulated oven
Storage Temperature	21°C	21°C	60°C

The results of comparing Group 1A and Group 1B will be used to investigate the effect of the amount of intial volatile matter content on shrinkage behavior of EPS foam. Comparing Group 1A and Group 2 will reveal the influence of high temperature storage conditions on the shrinkage behavior. These three groups together can help isolate which factors contribute more than others to the shrinkage and ultimately dimensional stability of EPS foam.

3.3 Phase Transitions and Crystallinity

3.3.1 Background

Differential scanning calorimetry (DSC) was applied to eliminate the effect of material crystallinity by confirming the polystyrene in the EPS used in this study was amorphous. DSC is used to determine thermal transitions by measuring the heat absorbed. It can provide the glass transition temperature (T_g), crystallization temperature (T_c), and melting temperature (T_m) of a material of interest, as shown in *Figure 19* below.

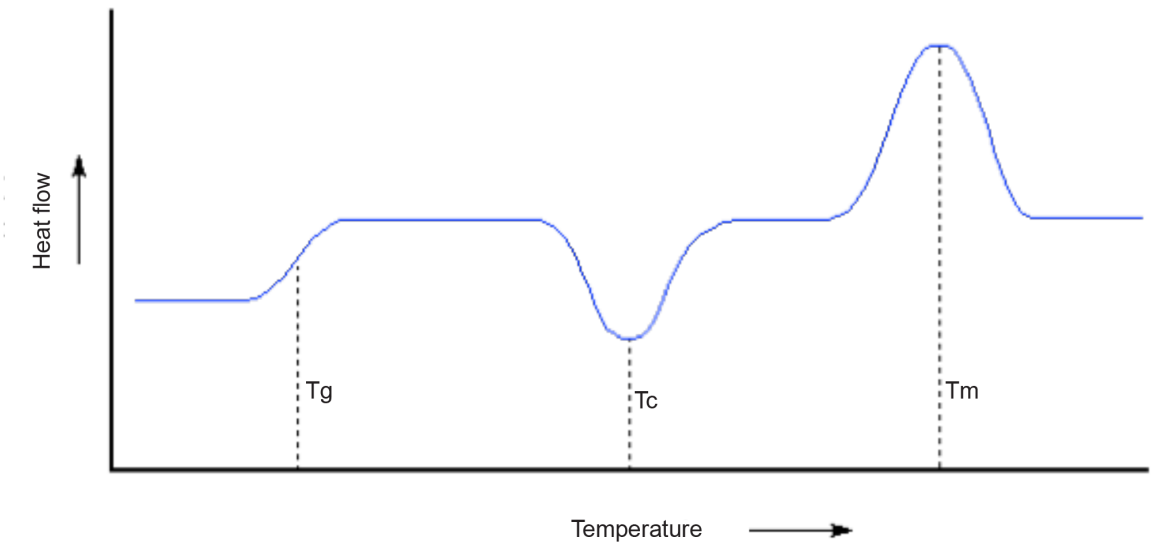

Figure 19: A typical DSC curve showing the glass transition temperature, crystallization temperature, and melting temperature peaks. [2]

However, the T_c and T_m peaks are only seen if the material is crystalline. Most commercially-used polystyrene is atactic, meaning it has no order to which side of its chain phenyl groups attach, and thus amorphous. Atactic polystyrene is produced with free radical polymerization, and is cheap, easy, and quick to make, thus very often used in industry. Polystyrene could also, however, be syndiotactic, meaning phenyl groups attach to alternating sides of the polymer backbone chain to produce a crystalline material. The two types of polystyrene are visually shown in *Figure 20* below. This syndiotactic type of polystyrene is produced with metallocene polymerization, which is significantly more expensive than producing atactic polystyrene, and has melting temperature of 270 °C. There exists also a third type of polystyrene, isotactic

polystyrene, but this type is rarely used in industrial applications, and therefore was assumed to not be present in the EPS samples in this study [2, 8].

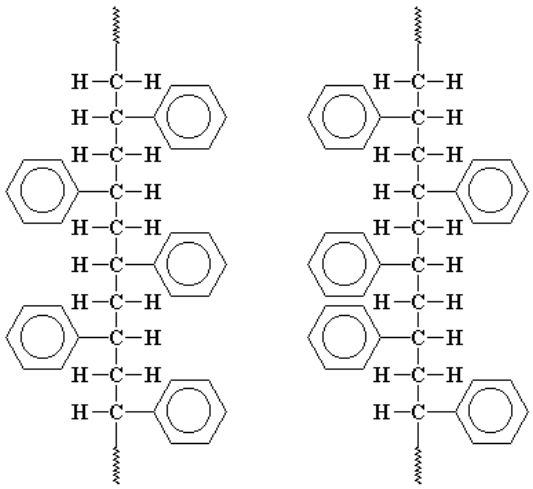

Figure 20: The difference in structure between syndiotactic (left) and atactic (right) polystyrene. Syndiotactic polystyrene's regular arrangement allows for crystallinity, whereas atactic polystyrene is fully amorphous. [8]

DSC was used to determine the glass transition temperature of the EPS material in this study, as well as to test if it was made with fully amorphous or rather semi-crystalline polystyrene. Semi-crystalline polystyrene would be possible if BASF uses syndiotactic polystyrene in its raw material Peripor microgranular beads. Its production is quite expensive because it is made with metallocene catalysis polymerization rather than merely free radical polymerization like the commonly-used atactic, amorphous polystyrene. Because of its crystallinity, syndiotactic polystyrene retains the blowing agent for a longer amount of time. The orderly packing nature of the atoms makes the crystalline structure less conducive (compared to the more free atoms of an amorphous

structure) for residual blowing agent molecules to diffuse out after processing. Therefore, it would be attractive as a producer to include syndiotactic polystyrene for longer raw material microgranule warehouse storage possibilities, with a trade off of the extra high cost compared to atactic polystyrene.

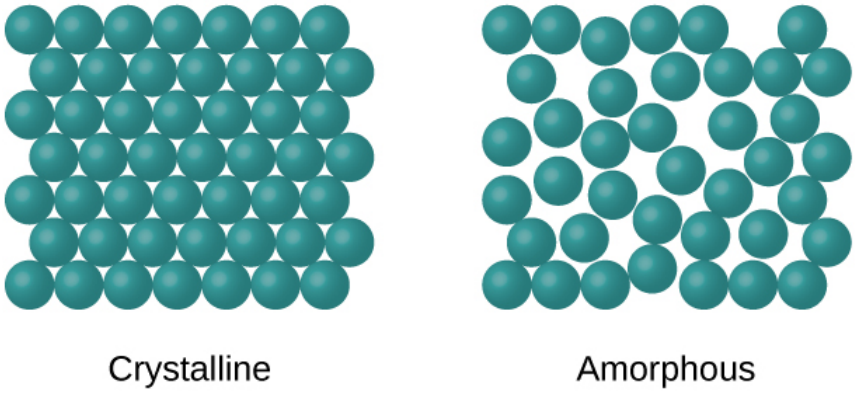

Figure 21: The difference in atomic packing between crystalline (left) and amorphous (right) solids. Syndiotactic polystyrene's regular arrangement allows for crystallinity, whereas atactic polystyrene is fully amorphous. [1]

Additionally, the T_g is known to decrease with increasing amount of volatiles for EPS. The T_g of pure polystyrene is 100 °C, but decreases with more volatile matter content. Therefore, the phase transitions measurements with DSC were also used to determine the T_g of the raw material microgranules used in this study.

3.3.2 Testing Methodology

To find out if the polystyrene used in this study had any amount of crystallinity, the microgranules from both types of raw material were tested with DSC. Both the "new" and "old" microgranule samples were tested three times to obtain statistically significant

values. A Mettler-Toledo instrument was used, following a method that heated each sample twice from 25-310 °C at a rate of 10 K/min with nitrogen gas in an inert atmosphere. A final temperature of 310 °C was chosen because it is well above the melting temperature of sydniotactic PS, which is 270 °C. Thus, if the microgranules in this study contained any amount of syndiotactic, crystalline polystyrene, a melting peak around 270 °C should be observed. The second heating curve was examined for the presence of T_c or T_m peaks because the first heating cycle is used to evaporate the volatile matter in the EPS. After the volatiles evaporate, the leftover polystyrene material is analyzed from the results of the second heating cycle for crystallinity.

3.3.3 Results

After testing both the “new” and the “old” microgranules, every sample tested obtained a second heating curve following the same shape as the one shown below in *Figure 22*.

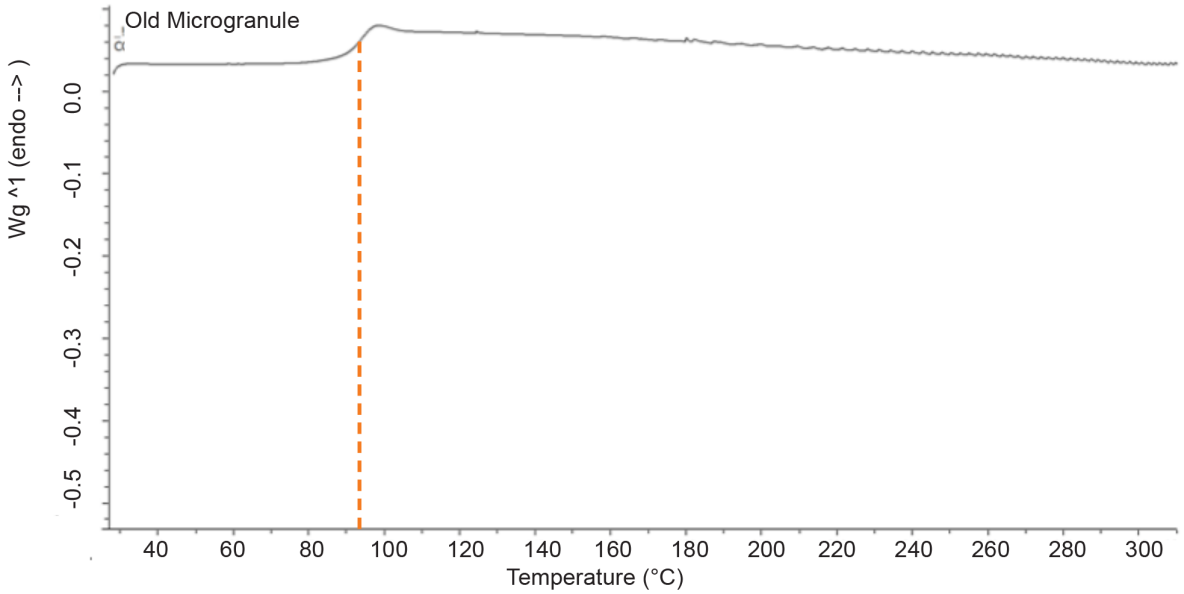

Figure 22: DSC curve for a raw material "old" micrograniule, showing a clear Tg (marked) but no T_c or T_m peaks. [Author]

In every measurement for both the "new" and "old" microgranules, a clear glass transition temperature shift was seen near the polystyrene T_g of 100 °C, but no other peaks were measured. The specific value of the T_g was evaluated as the midpoint of this area of shift in the second heating curve. Both microgranules showed similar T_g values: for "new" microgranules, the average T_g was calculated to be 95.2 °C; for "old" microgranules, the average T_g was 94.3 °C. The *Table 5* below elaborates upon the values obtained for T_g per sample each time it was run through a DSC cycle.

Table 5: T_g measurements for all microgranule samples tested with DSC. [Author]

Sample	T_g (°C)
Mikro_new_1	94.92
Mikro_new_2	94.12
Mikro_new_3	96.48
"New" Microgranules Average	**95.17**
Mikro_old_1	93.32
Mikro_old_2	94.34
Mikro_old_3	95.25
"Old" Microgranules Average	**94.30**

Additionally, no clear T_c or T_m peaks were observed in the second heating cycle to signify crystallinity, or the presence of syndiotactic polystyrene. If there was any syndiotactic polystyrene at all present in the EPS material used in this study, its amount was too low to have an impact on foaming or storing behavior, or else it would have been clearly detectable with the DSC trials. It is unlikely that there was any syndiotactic polystyrene within the microgranules also because of its high production cost compared to atactic polystyrene, and it would not be worth putting in such a small amount that

makes no different to the material performance. Thus, the EPS in this study was found to be fully amorphous, atactic polystyrene.

3.4 The Effect of Volatile Matter Content on EPS Shrinkage

3.4.1 Background

After processing, volatile matter from the blowing agent remains within EPS, affecting its shrinkage and thus dimensional stability. After processing, the residual blowing agent remaining within individual cells condenses. This causes a partial vacuum and leads to dimensional instability, because the cell structure is not strong enough to resist the excess pressure of the atmosphere over that within the cells [13, 35]. Therefore, the content of volatile matter in EPS plates was tracked in this study with TGA and further analyzed qualitatively by gas chromatography coupled with mass spectrometry (GC-MS) to learn the composition of the matter.

Twelve samples from Group 1A and twelve samples from Group 1B were dedicated to TGA testing for the entire duration of time. Each time, three of these twelve plates were measured, alternatively cycling through each of the samples. Measurements were taken once per week once the molded parts were made for 61 days. Prior to molding, TGA measurements were also taken of the “New” and “Old” microgranules and pre-foam materials (refer to Table 2 for definition of “New” and “Old”). From Group 2 (high-temperature storage plates), one sample was removed from the oven at each time interval and tested at three points with TGA in addition to all of

the previously removed Group 2 plates. Three points were chosen to test per measurement point in order to minimize the instrument use because of its time and availability constraint, while also still obtaining statistically significant values.

3.4.2 Testing Methodology

The volatile matter content of the EPS material in this study was measured primarily using TGA, which measures the changes in the physical and chemical properties as a function of increasing temperature (with constant heating rate) or a function of time (with constant temperature) for materials which exhibit a loss of volatiles. Testing was done using a Mettler-Toledo instrument, with which samples were heating from 25-130 °C at a rate of 10 °C per min, then held at 130 °C for 10 minutes during which the weight loss was measured as volatiles diffused out. The TGA testing was done periodically at various points before, during, and after processing, following approximately the same frequency as the dimensional testing to allow for comparison of final data.

Since TGA gives the amount of entire volatile matter inside a material, GC-MS was also performed periodically to analyze the exact make-up of the volatile matter. This technique is used for the analysis and quantification of organic volatile and semi-volatile compounds. The gas chromatography portion is used to separate a mixture into individual components with a temperature-controlled capillary column. Small molecules with lower boiling points travel faster down the column, and are thus separated and detected sooner than larger molecules. The MS portion then identifies the individual

components from their mass spectra [Evans Analytical Group, Bristol Univ]. An Agilent Technologies 5977A MSD instrument with an Agilent Technologies 7890B gas chromatography (GC) system was used in this study. Helium was used as the carrier gas, and a quadrupole mass analyzer was used as a detector for the mass spectrometry (MS) portion. Testing was done qualitatively, to be coupled with TGA results in order to determine quantitative amounts of specific substances within the volatile content of EPS.

3.4.3 Measurement of Volatile Matter Content

Testing with TGA, curves like the one below in *Figure 23* were obtained showing the weight percent (compared to the starting mass of the inserted sample) of EPS over temperature.

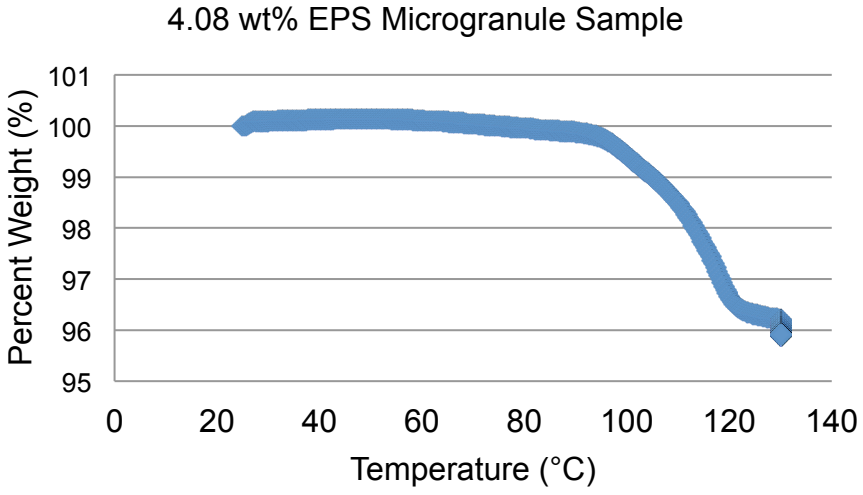

Figure 23: Example of volatile matter content curves obtained from TGA testing, showing volatile matter content over temperature. The weight loss starts at 90° C and ends at 120° C. The T_g was measured by DSC to be 94.3° C, Section 3.3. [Author]

The curve is an example of a TGA test done on an “old” microgranule sample, showing weight loss beginning at approximately 90 °C and ending at approximately 120 °C. This “old” microgranule sample lost approximately 4% of its weight during heating, corresponding to its volatile matter content. The weight loss begins at a temperature above the normal boiling point of the compounds which make up the volatile matter, as determined by GC-MS. This occurs because the compounds are trapped within the solid polystyrene cells and only come out around the T_g of the polystyrene (94.3 °C, as determined by DSC), after the polymer has softened.

The values measured for volatile content by TGA were then plotted with respect to time for each of the sample groups for comparison. Group 1A and Group 1B samples were plotted together to see the effect of initial volatile matter content on final volatile matter content. Group 1A and Group 2 samples were plotted together to learn the effect of high temperature storage on final volatile matter content. The results are shown below.

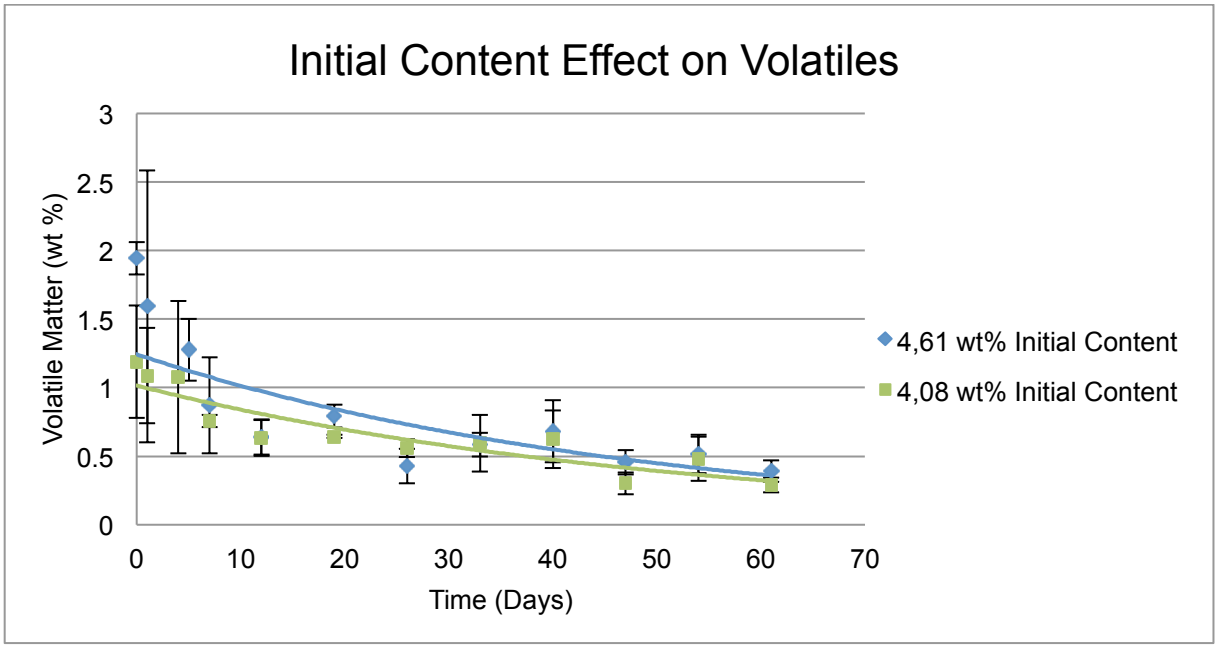

Figure 24: Volatile matter content of Group 1A and 1B over time, used to compare the effects of initial volatiles amount on final volatiles amount. The starting point of 0 is taken as 24 hours after de-molding. [Author]

The zero point on this graph is taken as 24 hours after de-molding of the EPS plates to allow for stabilization by cooling of the parts. Fit lines are added to guide the eye through the points measured. Prior measured points for Group 1A and Group 1B of the microgranule and pre-foam material volatile content, measured before and during processing are shown in *Table 6* below.

Table 6: Volatile matter content of samples prior to molding. Note that "stabilizing" refers to the 48 hours that samples were stored in silos between the pre-foam step and the steam-chest molding step. [Author]

	Group 1A		Group 1B	
Processing Step	**Volatile Matter Content (wt%)**	**StDev**	**Volatile Matter Content (wt%)**	**StDev**
Microgranules	4.61	0.02	4.08	0.03
Pre-foam (pre-stabilizing)	2.75	0.10	2.28	0.09
Prefoam (post-stabilizing)	1.81	0.07	1.01	0.14

From *Figure 24* above, we see that despite the different amounts of volatile matter in each of the group's raw material microgranules (Group 1A with 4.61 wt% and Group 1B with 4.08 wt%), at the end of the duration of this study, both groups end up with approximately the same amount of volatiles. This shows that the initial amount of volatile matter in the raw material microgranules does not seem to affect significantly the amount of volatile matter in the molded parts over time.

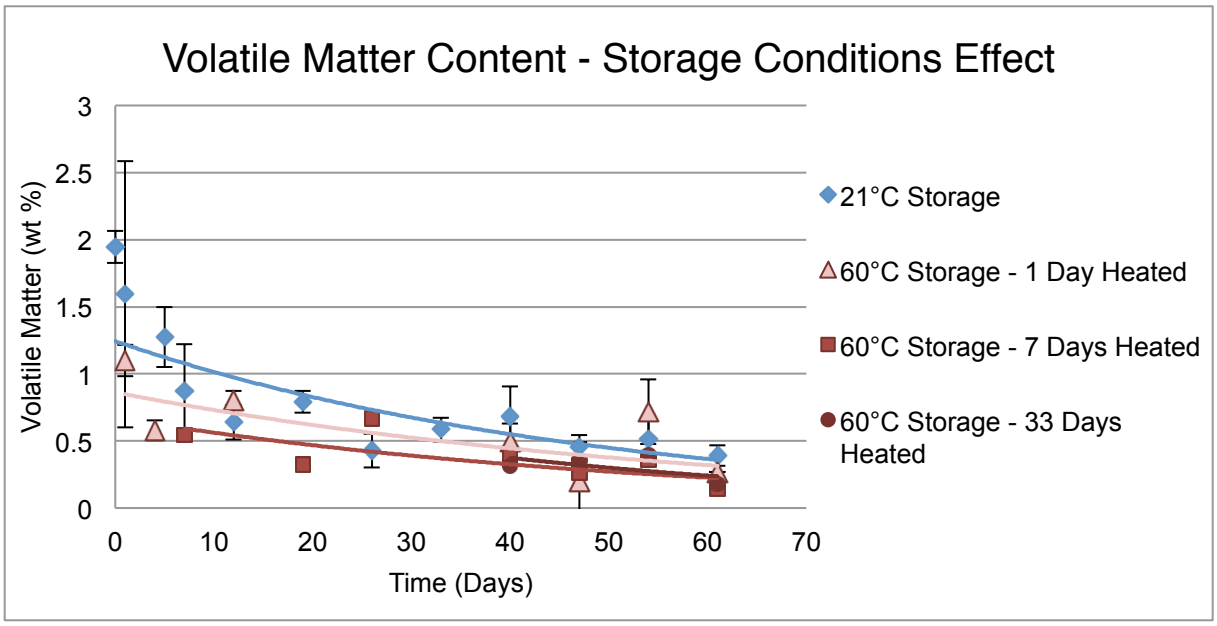

Figure 25: Volatile matter content of Group 1A and 2 over time, used to compare the effects of a high storage temperature on final volatiles amount. The starting point of 0 is taken as 24 hours after de-molding. [Author]

The zero point on the graph in *Figure 25* is taken as 24 hours after de-molding of the EPS plates to allow for stabilization by cooling of the parts. Fit lines are added to guide the eye through the points measured. Three different sections of Group 2 samples are shown here, one group heated just 1 Day, another group heated 7 Days, and another group heated for 33 days. After the 1, 7, or 33 days in the oven, the samples were stored at 21 °C with Group 1A and Group 1B samples, and the volatile matter tracking began. Thus, the data for those samples stored 7 days in the oven begins at a time of 7 days and not earlier. All of the samples from Group 2 heated in the oven at 60 °C show lower volatile matter content during the earlier days of the trial. This is because higher

storage temperature, leading to less leftover matter while the oven storage. Increasing the temperature increases the diffusion of small, high-energy gas molecules, meaning molecules move out of the entire plate faster [Castro, Vilaplana], as seen in the difference between Group 2 volatile matter and Group 1A. For instance, at Day 19, Group 1A samples had an average of 0.79 wt% volatile matter, while 7-day-heated-Group 2 samples had an average of 0.32 wt% volatile matter. However, by the end of the trials, all samples stored in the oven, regardless of the duration of time heated, reached approximately the same amount of volatile matter content. From the dimensional shrinkage measurements, presented in Section 3.6, it was found that only the samples in Group 2 were found to reach stability by the end of the duration of the trials. This leads to the conclusion that the amount of volatile matter content in EPS foam is not the final influencer of dimensional stability.

3.4.4 Qualitative Composition of Volatile Matter

EPS samples were also measured with GC-MS at different points along the foam production and lifespan to track the distribution of how specific compounds within the volatile matter change over time. The volatile matter content is known to be made up of mostly pentane from the blowing agent used to expand the EPS, but GC-MS tests were conducted to see the changes in the specific distribution of other compounds along the processing and post-processing lifetime of the material. This data can then be used with dimensional measurements to evaluate the volatile matter composition effect on EPS stability. The testing was conducted at various points based on the timing and

availability of the GC-MS instrument. The Group 1A and Group 2 samples were tested at five points, while the Group 1B samples were tested at four points along the lifetime of the foam during the course of this study.

Qualitative measurements of the amount of each compound relative to the others within the volatile matter makeup were obtained for each sample. First, using gas chromatography, the peak intensity distribution was analyzed, such as for instance the one shown below in *Figure 26*.

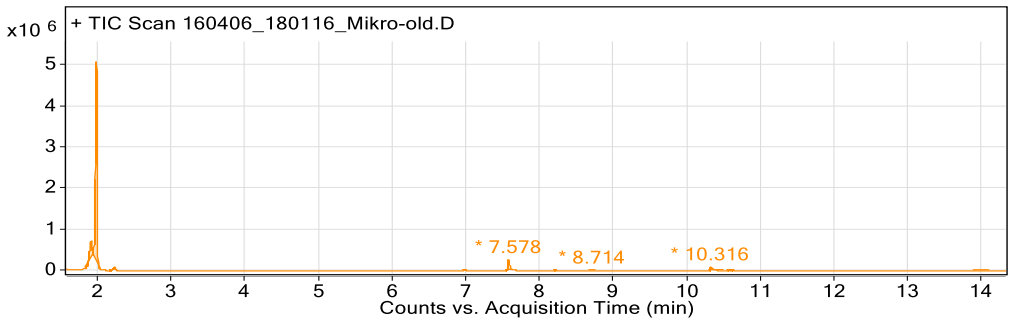

Figure 26: Peak intensity distribution of "Old" microgranules using GC-MS. [Author]

According to their boiling point and molecular size, the molecules of various volatile matter travel through the capillary column at different speeds. This thus affects the rate at which they are detected, and the peak maps shown above are further analyzed with MS. First, an integration peak list, such as *Table 7*, is produced.

Table 7: Integration peak list of "Old" microgranules using GC-MS. [Author]

Peak	Start	RT	End	Area	AreaSum%
1	1.831	1.922	1.942	766101.63	7.77
2	1.945	1.991	2.046	8183281.23	83.04
3	2.205	2.231	2.259	101700.24	1.03
4	6.952	6.989	7.021	33372.37	0.34
5	7.536	7.578	7.64	460287.77	4.67
6	8.19	8.213	8.236	11274.39	0.11
7	8.667	8.714	8.764	16463.38	0.17
8	10.293	10.316	10.501	237239.57	2.41
9	10.544	10.614	10.639	29138.29	0.3
10	13.885	14.024	14.107	15723.04	0.16

The integration peak list lists the area of each peak, and thus the software calculated the amounts of each peak relative to all other peaks detected by the instrument. The MS portion of the analysis was further used to identify each of the peaks to a specific compound based on the counts versus mass-to-charge graphs, similar to *Figure 27* below.

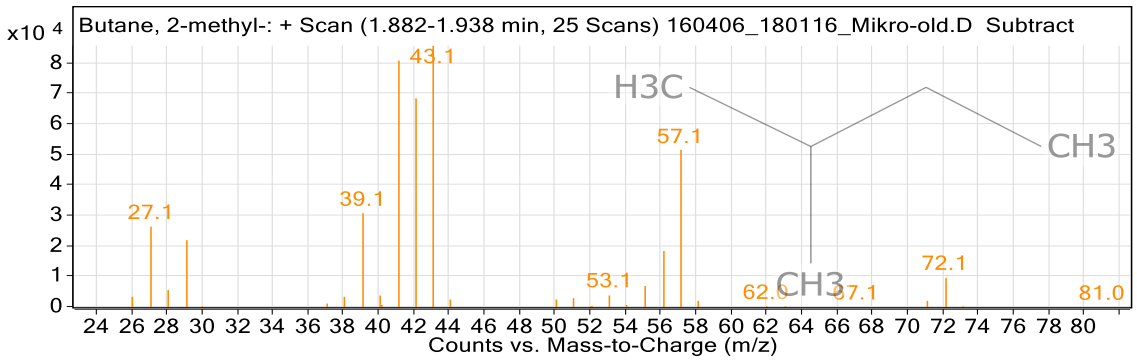

Figure 27: Identification of particular peak in "Old" microgranules. [Author]

The instrument software compared peak distribution to its library of compounds to identify the distribution of volatile matter. When a compound of matching peak distribution was found, the identity of the volatile matter was determined, as shown in *Figure 28* below as an example.

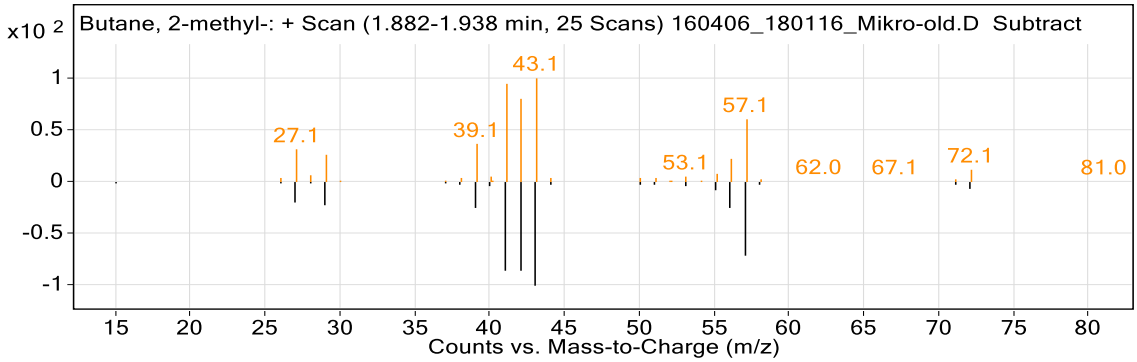

Figure 28: Comparison of intensity distribution of particular peak to library spectrum to identify compound identity in "Old" microgranules. [Author]

The results of the samples tesed in all groups is presented in *Table 8* below, showing all the compounds that made up the volatile matter at various points in the experimentation timeline. A prior-made EPS Peripor 300E sample was also tested in order to see what

the volatile matter distribution was in a fully stable sample, and thus see which compounds do not affect EPS shrinkage in the long term.

Table 8: Composition history of volatile matter in each of the sample groups (continued until page 79). [Author]

Group 1A	**Volatile Matter Composition (%)**				
	Microgranules	**Pre-foam (pre-stabilization)**	**Pre-foam (post-stabilization)**	**Day 19**	**Day 61**
Isopentane	9.51	17.69	19.19	55.415	88.30
n-Pentane	81.97	74.99	65.82	19.6	0
1-Pentene	0.50	0.52	0.56	0	0
Ethylbenzene	0.88	1.15	2.22	3.825	0.80
Styrene	4.10	4.03	8.63	12.76	2.30
1-Methylethyl-benzene (Cumene)	0.24	0.41	0.68	1.515	1.60
2-Propenyl-benzene	0.05	0	0	0	0
Propyl-benzene	0.23	0.22	0.62	5.07	0
Acetophenone	2.02	0.69	1.58	0.43	2.78
1-Methoxyethyl-benzene	0.29	0.31	0.69	1.38	0
1-Difluoro-2-methyl-3-ethyl cyclopropane	0	0	0	0	1.45
Isopropyl alcohol	0	0	0	0	2.775

Group 1B	**Volatile Matter Composition (%)**			
	Microgranules	**Pre-foam (post-stabilization)**	**Day 19**	**Day 61**
Isopentane	7.77	23.03	58.92	69.11
n-Pentane	83.04	66.91	33.915	3.25
1-Pentene	1.03	1.04	0.95	0.98
Ethylbenzene	0.34	0.49	1.14	1.05
Styrene	4.67	6.27	11.03	10.00
1-Methylethyl-benzene (Cumene)	0.11	0.53	1.255	1.15
Propyl-benzene	0.17	0.26	0.285	0.84
Acetophenone	2.41	1.05	5.115	9.80
1-Methoxyethyl-benzene	0.30	0.41	1.84	1.92
Dicumyl peroxide	0.16	0	0	1.90

Group 2	Volatile Matter Composition (%)				
	Micro-granules	**Pre-foam (pre-stabilization)**	**Pre-foam (post-stabilization)**	**Day 19**	**Day 61**
Isopentane	9.51	17.69	19.19	73.56	84.16
n-Pentane	81.97	74.99	65.82	15.81	0
1-Pentene	0.5	0.52	0.56	0	0
Ethylbenzene	0.88	1.15	2.22	0	2.3
Styrene	4.1	4.03	8.63	0	2.55
1-Methylethyl-benzene (Cumene)	0.24	0.41	0.68	1.41	1.96
2-Propenyl-benzene	0.05	0	0	0	0
Propyl-benzene	0.23	0.22	0.62	0.705	0.88
Acetophenone	2.02	0.69	1.58	5.015	3.33
1-Methoxyethyl-benzene	0.29	0.31	0.69	0	0
1-Difluoro-2-methyl-3-ethyl cyclopropane	0	0	0	0	0
Isopropyl alcohol	0	0	0	0	0
Dicumyl peroxide	0	0	0	0	2.28
1-Methyl-1-phenylethyl hydroperoxide	0	0	0	3.5	2.53

In all of the sample groups, most pentane (n-pentane and isopentane) was measured throughout the foam material lifetime, in agreement with prior studies and the blowing

agent content. In *Table 8*, the isopentane amounts are highlighted in blue, while the n-pentane amounts are shown in red to allow for easy following of the compositional change of these two compounds. This pentane is residual blowing agent left over from the foam expansion process. Other compounds that were measured, all at relatively very small amounts, were all high molecular weight compounds used either in the raw material production or contaminants. The contaminants could have come into contact with samples throughout storage and transportation across various surroundings. Acetophenone was seen in all samples tested, and is commonly used as a special solvent for plastics and resins, as well as a catalyst for olefin polymerization [48]. Cumene was also present, which is used in the manufacturing of acetophenone. The compound also often forms peroxides, which were seen in samples at later measurement points, after storage in contact with air [46]. Ethyl benzene is used in styrene manufacturing, whereas isopropyl alcohol (IPA) was most likely caused by contact of some samples with surfaces that were cleaned with IPA-containing cleaning supplies [47].

A prior-produced (over 1 year ago, with the same production conditions) Peripor 300E EPS plate was also tested with the same GC-MS procedure, and produced a very similar distribution of the compounds making up the volatile matter remaining within.

Table 9: Composition of volatile matter in a prior-produced EPS Peripor 300E sample over time. [Author]

>1 Year Old EPS Plate	**Volatile Matter Distribution (%)**
Isopentane	62.91
n-Pentane	2.39
Ethylbenzene	4.46
Styrene	2.54
1-Methylethyl-benzene (Cumene)	3.81
Propyl-benzene	1.76
Acetophenone	9.54
1-Methoxyethyl-benzene	9.27
Dicumyl peroxide	3.32

The purpose of testing this prior-produced sample was to see which compounds remain in EPS after it has completely stabilized according to the industry standard, and hence which compounds have no effect on the shrinkage of the the same material. Its very similar distribution of volatile matter to the new EPS plates produced for this study showed that after a certain point, the volatile matter content no longer affects dimensional stability.

From the GC-MS results, the largest shift in the distribution of volatiles noticeably came from the fastest diffusing out of n-pentane, thus isopentane becoming the majority

compound in the volatile matter makeup as time went on. The combination of GC-MS and TGA results plotted onto the same plots, shown below in *Figure 29*, allow for visualization of the shift of the portions of isopentane (shown in blue) verses n-pentane (shown in red) in the volatiles over time for all three groups of samples, plus the other contents in various shades of grey.

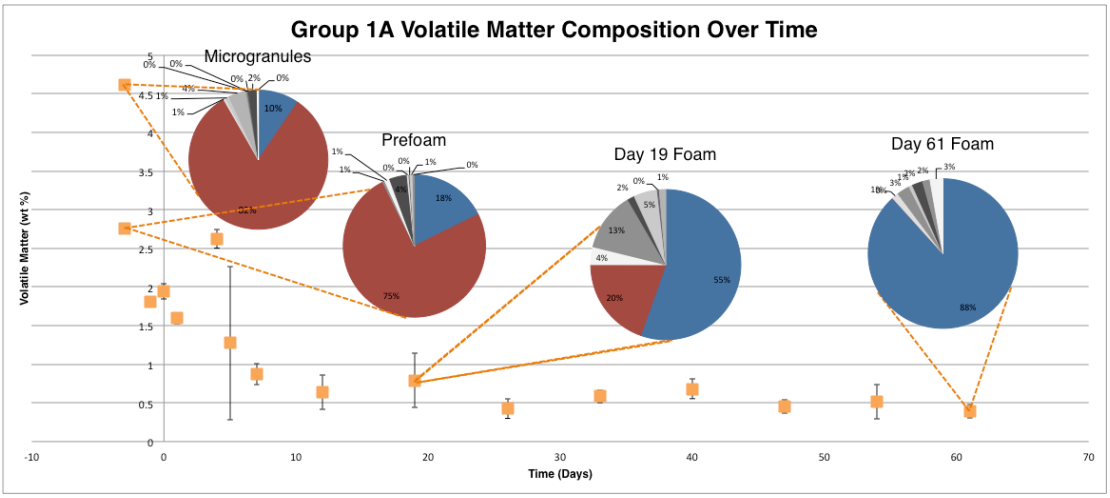

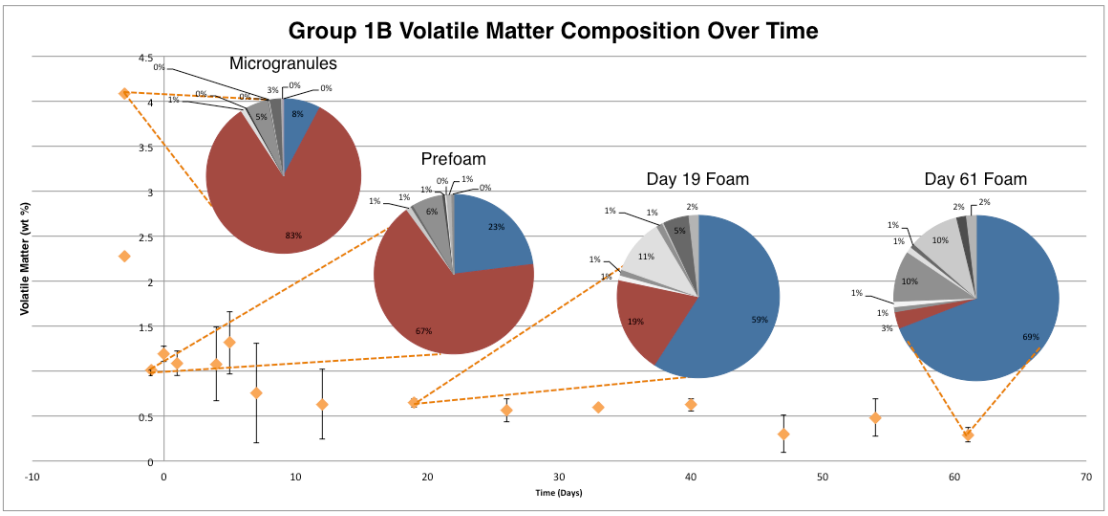

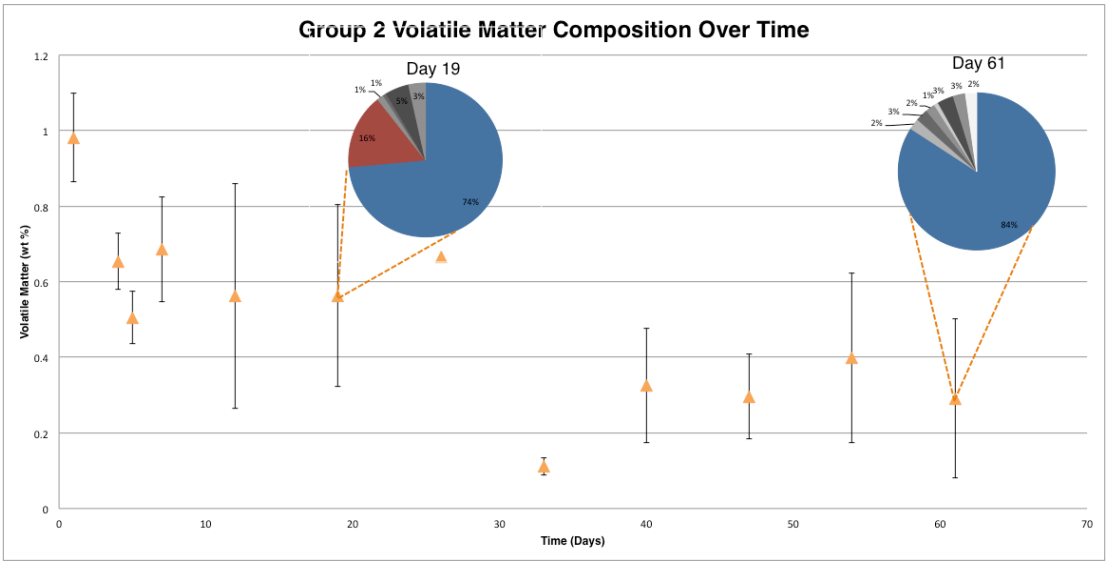

Figure 29: Comparison of volatile matter over time, with n-pentane, (red) isopentane (blue), and other volatiles (greys). [Author]

Both the “old” and “new” microgranules started with approximately 80% of the volatiles as n-pentane, as per agreement with the BASF 300E Peripor date sheet [51]. This n-pentane is the primary compound in the blowing agent, and is used to expand the microgranules into cellular foams during the steam-chest molding process. The proportion of the n-pentane and isopentane, however, change over the time. The graphs below in *Figure 30* highlight these drastic compositional changes over time, with n-pentane showin in red and isopentane in blue.

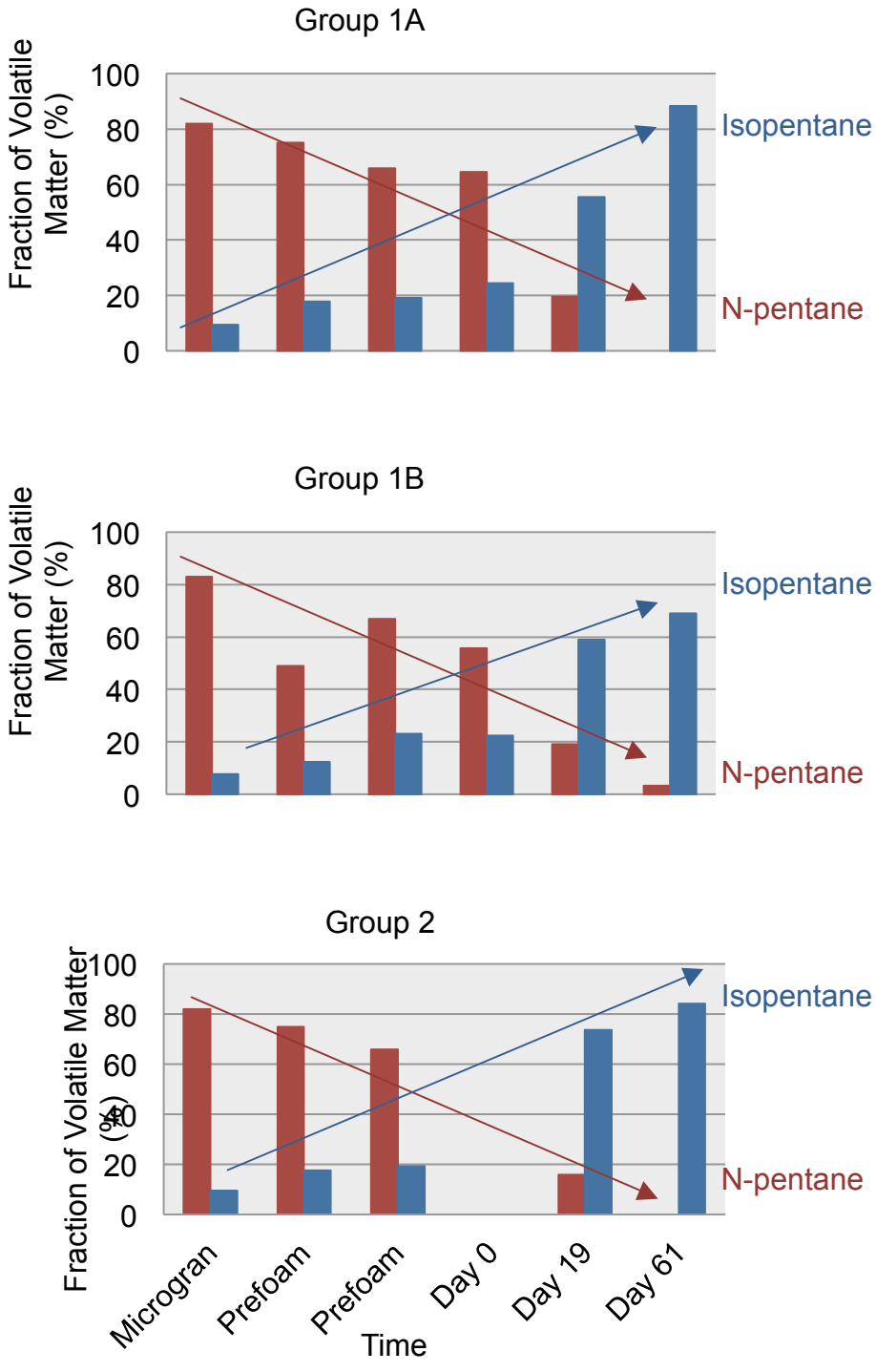

Figure 30: Relative comparison of the two types of pentane in the volatile matter over time. N-pentane composition is shown in red and isopentane in blue. [Author]

In all three groups, a majority of isopentane rather than n-pentane is seen at the end of the trials. This could be attributed to the more branch-like molecular shape of isopentane compared to the simple, long n-pentane. This makes it easier for n-pentane molecules to diffuse out of the foam faster than isopentane moleucules. The point at which the entire volatile matter content of the material drops below 1 wt% is when n-pentane no longer is the major compound in the volatiles. Additionally the samples from all three groups end up with approximately the same distribution of volatile matter content by the end of the trials (61 days after de-molding). However, only the oven-stored plates reached stability in that time according to DIN EN 1603. Thus, the volatile matter content below 1 wt%, the point at which isopentane becomes the majority of volatile matter, does not seem to affect EPS shrinkage. After this point, air diffusion into cells becomes more important, and becomes the determining factor for dimensional stability.

3.5 Residual Stress Measurement Methods for EPS Foam

3.5.1 Background

Residual stresses develop during most manufacturing processes due to material deformation, machining, heat treating, or processing that changes the shape or properties [33]. Rapid cooling of the mold during EPS processing leads to faster surface solidification before the core. Because of thermal contraction, the core shrinks with more cooling, as illustrated in *Figure 7* in Section 1.3. However, the shrinkage is

constrained by the already-cooled solid outer region, resulting in tensile residual stresses in the core balanced by compressive stresses in the skin. Residual stresses are generally undesirable, as they increase the risk of dimensional instability, lead to environmental stress cracking, and decrease life expectancy of materials [42]. Thus, in order to see if the polymer matrix behavior also plays a role in post-processed dimensional stability of EPS, residual stress testing was performed to track stresses over time after molding. As there is not any prior literature on residual stress measurement of EPS polymer foam, the main purpose of the residual stress measurement of this study was to establish a method to determine the residual stresses in EPS foam from the available methods of residual stress measurement techniques. Then, if any methods were able to measure residual stresses in the foam, the next step was to determine if the stresses are significant enough to affect the post-processed shrinkage behavior. Based on the amorphous polymer material and flat plate shape of the EPS samples used in this study, three possible types of residual stress testing methods were employed: hole drilling method, Raman spectroscopy, and curvature layer removal method. The frequency and timing of the tests performed were based on the accessibility and success of the available instruments and measurement methods.

3.5.2 Residual Stress Measurement Methods

Measurement of residual stresses in materials is done either by measuring the actual strain or the changes in strain [70]. Besides, a variety of measurement methods exist for detecting residual stresses, depending on the type of material, its shape, and

the desired measurements. However, only more in-depth methods such as x-ray diffraction, synchrotron, and Raman spectroscopy can be used to measure micro residual stresses in the microstructure, in addition to the measurable macro ones.

The birefringence method measures changes in optical properties of a polymer that are caused by residual stresses present. It is, however, limited to transparent materials [42]. A chemical probe method can also be used to detect residual stresses in materials by applying chemical to the surface and measuring the time taken to fracture. This method is limited by its ability to only detect tensile stresses [42]. Photo-stress coatings give a qualitative measurement, showing locations of high stresses but the stress is unknown. X-ray diffraction, on the other hand, gives quantitative measures of residual stresses that are closest to the surface of materials. However, the material must be crystalline and in a thin shape [70].

The layer removal method measures the degree of curvature introduced into a flat plate sample by removing thin layers from the surface. It determines the strain and hence residual stresses present in the layer that has been removed, as the plate bends with a curvature dependent on the original stress distribution in the removed layer and elastic properties of the remaining plate [33, 42, 66]. The curvature can be measured with optical microscopy, laser scanning, strain gages, or profilometry [33]. The layer removal method is often the primary method for measuring residual stresses in plastics, but it can only be applied to flat plate samples and cannot measure very near-surface stresses [33, 42, 66].

The hole drilling method relieves local residual stresses by drilling a hole onto the surface of samples and then measures the resulting strain around the hole which reflects the residual stresses [42]. For this method, high speed drilling is necessary to avoid introducing new stresses to the specimen, while the maximum possible depth is limited by 2/3 the hole diameter [33, 70]. It assumes the material to be isotropic and linear elastic, the stresses to not vary much with depth, and small stress variations within the hole. Incremental hole drilling can be used to measure the stress profiles and gradients across a sample [33]. ASTM E387-99 outlines the standard hole drilling measurement method, but has been often altered when applying to polymers and with new strain measurement methods [33, 60, 66]. Thus, the method is well established, but is limited by possible errors from localized drilling heating, limited strain sensitivity, and applies only where residual stress values are less than half the yield strength [33, 42].

The Raman spectroscopy method measures residual stresses in materials using the Raman effect, which involves the interaction of light with matter. Incident laser light is directed toward the sample, causing the bonds between atoms to vibrate. The scattered light is then analyzed with a Raman spectrum, which reveals crucial information about the sample's physical state and chemical structure. It measures surface strains, and is advantageous in the sense that it is non-destructive, non-invasive, and provides high spatial resolution [33].

Two different methods were used in this study to determine the possibility of measuring residual stresses in EPS foam, and discovering whether the polymer matrix

stress behavior plays a role in overall part shrinkage: hole drilling method and Raman spectroscopy.

3.5.3 Testing Procedure

For the hole drilling method, a hole was drilled in a sample to remove a piece of stressed material, forcing the remaining surrounding material to find new stress equilibrium. This re-arrangement of stresses causes a slight distortion in the surface of the sample near the hole, shown in exaggerated form in *Figure 31* below.

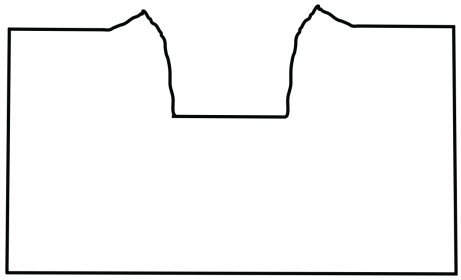

Figure 31: Cross-sectional view of exaggerated displacements around a hole drilled into a stressed material. These displacements are used to calculate the residual stresses. *[56]*

The displacements were measured and then used to calculate the residual stresses present in the sample before drilling. The hole is drilled with steps until it reaches a final designated depth, which has a maximum value of 2/3 the size of the drill bit diameter. Prism Electronic Speckle Pattern Interferometry (ESPI) was used to take laser images of the surface after each drilling step. In the setup, light from a laser source is split into two beams with a beam splitter. One part illuminates the object, which is imaged by a charged couple device (CCD) camera, and the other part passes through an optical

fiber directly to the camera. The setup used for the hole drilling method is illustrated below in *Figure 32*.

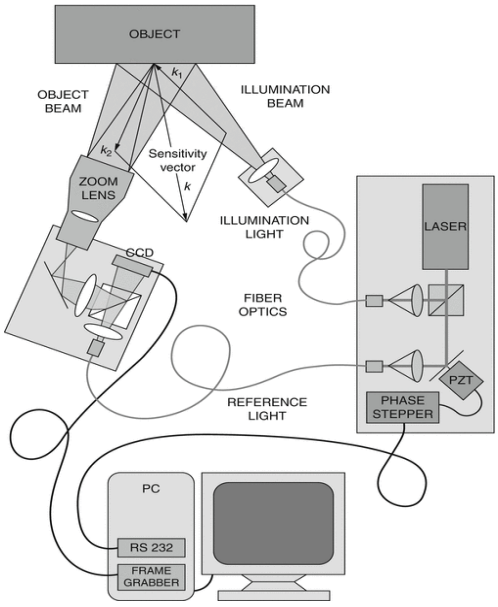

Figure 32: ESPI setup for residual stress measurements with the hole drilling method.

[55]

The two parts of the laser then interfere on the CCD surface to form a speckle pattern. The phase at each pixel of the CCD is then taken with imaging [Schaler]. Images were analyzed with the PrismS software to then calculate residual stresses present in each sample. The software follows the Integral Method and uses incremental referencing, and calculates sample depth profiles for the sample coordinate system (horizontal, vertical, and shear stresses), as well as the principal shear directions [Prism]. Samples in this study were drilled with a 3.2 mm diameter drill bit, as it was the largest size available, and the holes had a final depth of 1.9 mm.

The Raman spectroscopy uses the interaction of light with matter to learn about the physical and chemical properties of a material. Samples were illuminated with a laser beam, with the reflected light mapped onto a Raman spectrum to determine properties, as illustrated in *Figure 33* below.

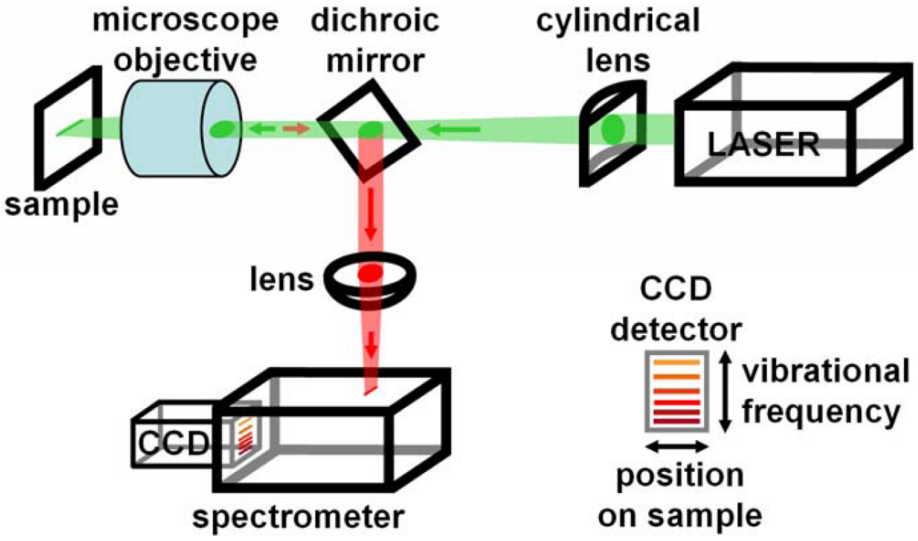

Figure 33: Raman spectroscopy setup for measuring residual stresses. [22]

Due to the lack of instrumentation available on site, EPS samples in this study were tested at the Leibniz Institute for Polymer Research in Dresden, Germany. There, a confocal Raman microscope combined with an alpha 300R (WITEC) imaging system was used with a 532 nm laser and a CCD detector behind a 600 g/mm grating. The EPS samples tested were cleaned from any dust particles before tesing using a stream of nitrogen.

3.5.4 Residual Stress Measurement Results

3.5.4.1 Hole Drilling Method

To measure residual stresses in EPS foam, this study began with the hole drilling method because it was the most readily available instrumentation on site. As the method is more commonly used for measuring residual stresses in metals, a run-through with a prior-produced (approximately 1 year old) Peripor plates was first conducted. These plates are known to have zero residual stresses because any residual stresses induced by thermal methods during fabrication would have been relieved since their production over a year ago. Therefore, if any residual stresses were to be measured, they were theorized to be the effects of the instrumentation rather than the material, and could then be subtracted from future tests with the plates produced for this study. The tests with the very old EPS plates results in the measurement of no significant amount of residual stresses measured, with all values between -0.3 – 0.3 MPa, as shown below in *Figure 34*.

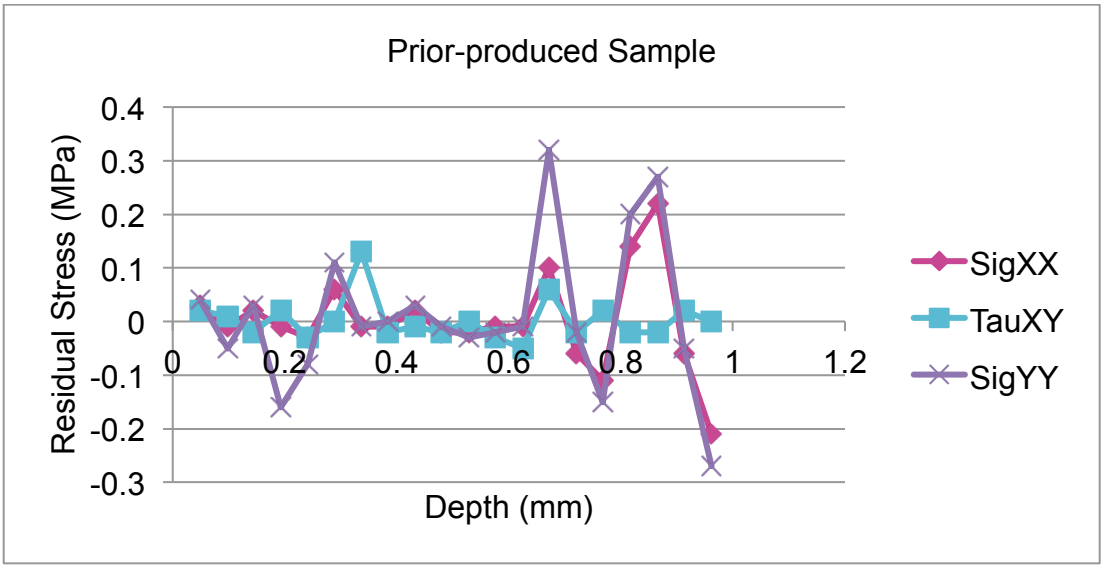

Figure 34: Results of hole drilling method for prior-produced sample, showing two-dimensional stress tensor at various drilled depths. [Author]

The graph in *Figure 34* shows the values of the two-dimensional stress tensor of the sample measured with respect to the hole depth drilled. With the extremely low values for residual stresses detected in the prior-produced EPS plates, it was therefore concluded that there were no instrumentation-induced residual stresses, and it would be worth testing new samples.

Two EPS plates, one cellar-stored and one oven-stored were measured at two different points of time shortly after de-molding: once at 1 day after de-molding, and a second time at 4 days after de-molding. The purpose of these days was to see if the residual stresses in the samples decreased ove time after de-molding, but points were still chosen close enough to de-molding to capture any thermal residual stresses that could have been caused by processing. Curves similar to the one below in *Figure 35*

were obtained for all samples, following no consistent pattern of peaks, and all at extremely low, near-zero MPa values.

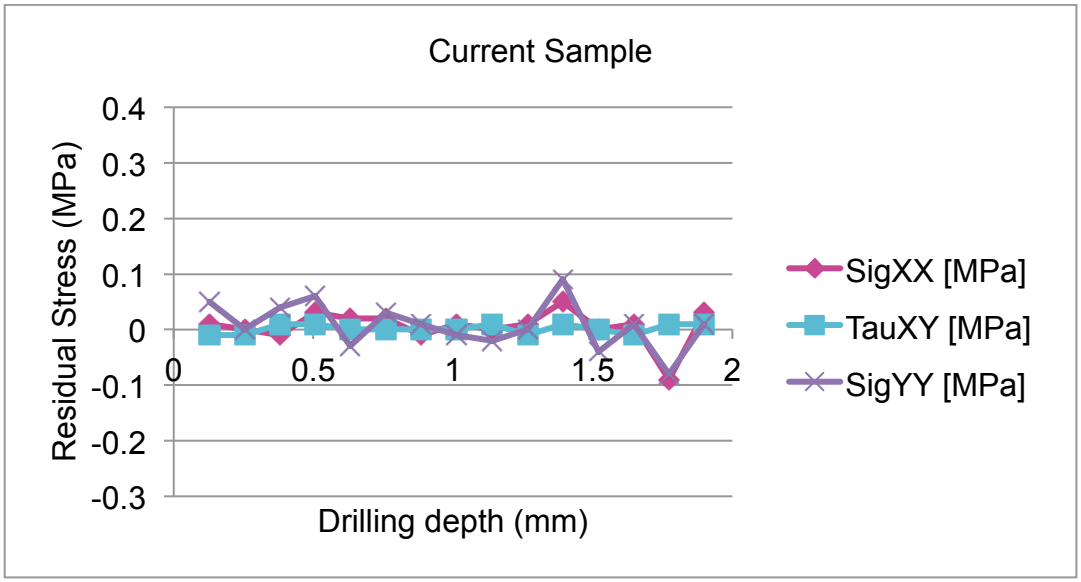

Figure 35: Results of hole drilling method for a current-produced sample for this study, showing two-dimensional stress tensor at various drilled depths. [Author]

The curves in *Figure 35* show the two-dimensional stress tensor values of the material measured as a function of depth drilled into the surface. All detected residual stress values were between -0.15 – 0.1 MPa, which were actually approximately half of those values detected for the prior-produced, one-year-old EPS plates. This was the opposite of what was expected, since the prior-produced samples were expected to have had all residual stresses caused by thermal processing conditions already relaxed in the past year. Based on these results, it was concluded that this setup of the hole drilling method that was used in this study cannot produce results with a known accuracy for a number

of possible reasons. First, the diameter of the hole drilled was approximately the same as the diameter of the cells of the foam, as shown below in *Figure 36*.

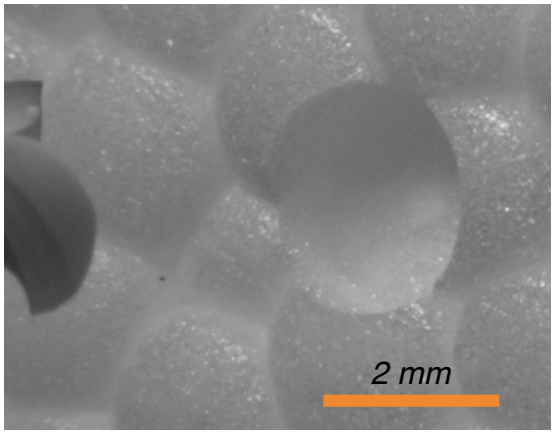

Figure 36: Illustration of similarity of drilled hole diameter size to foam cell diameter size. *[Author]*

Thus, the amount of material removed may not be enough to cause significant enough stress re-alignment displacement in the surrounding material. Additionally, as the hole depth was limited by the diameter of the drill bit, the amount drilled could have been too shallow to detect any residual stresses which exist below the near-surface of the material. As the specific Stresstech instrument used in this study is originally designed for use with metals (although stating in the manual it can be used for all types of materials, including polymers), the laser detectors could be not designed to be sensitive enough to completely accurately measure the low residual stress values in foams. Lastly, since the cell wall thickness in EPS foam is significantly lower than the cell bead diameter, the instrument could be unable to capture the effect of the polymer matrix because it is lost over the average area of the cells of the removed material which are

mostly filled with air. This is illustrated below in *Figure 37* with an SEM image of the material.

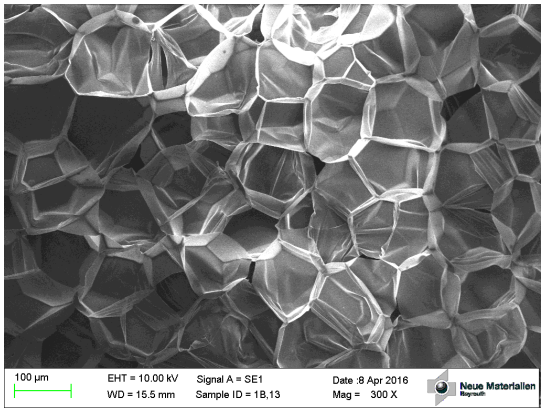

Figure 37: SEM image of EPS foam, highlighting large cell diameter compared to cell wall thickness. [Author]

3.5.4.2 Raman Spectroscopy

After detecting near-zero residual stress values by the hole drilling ESPI method, the samples were also tested with the Raman spectroscopy method. A prior-produced (approximately one year ago) Peripor plate was also tested to ensure no stresses were induced by the measurement method, similarly to the approach taken with the hole drilling method explained in Section 3.5.4.1. Samples were also tested 33 days after de-molding and 61 days after de-molding.

The resulting spectra showed the expected vibrations for polystyrene. However, there were no differences measured between the very old plates and the plates produced for this study, as shown below in *Figure 38*.

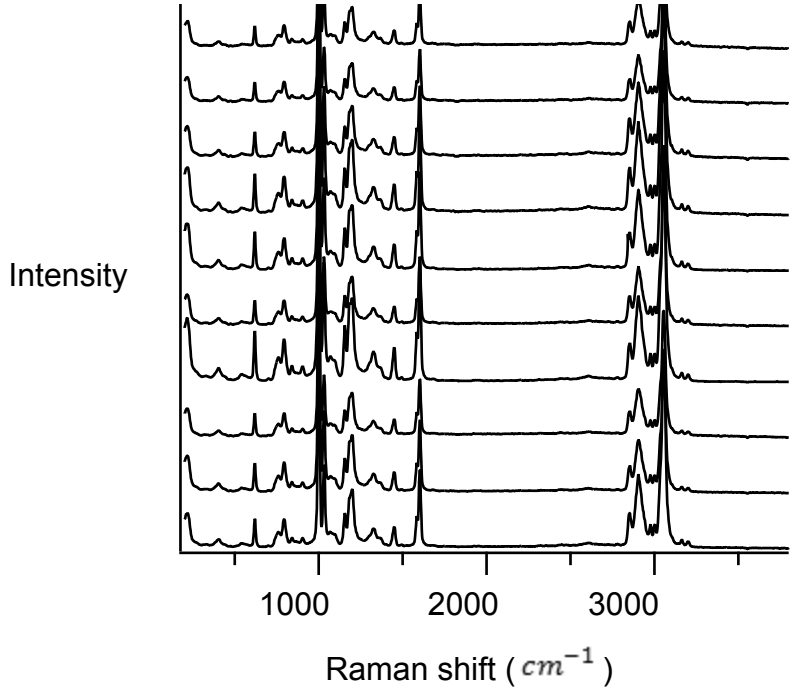

Figure 38: Raman spectroscopy results of very old Peripor sample (lowest 3 curves) tested in comparison to current produced samples (remaining curves). All samples produced the peaks for polystyrene, but there was no difference in residual stress detected. [Author]

The reason for the lack of the Raman spectroscopy method to detect residual stresses in the EPS samples could be for a number of reasons. The measurement might not have been sensitive enough to elucidate differences, the effects of the differences could have been lost by averaging over the measurement area of one square micron, or the residual stresses in the plates produced for this study were already relaxed a few weeks after processing and thus produced results similar to the very old plate.

3.6 Dimensional Shrinkage Tracking of EPS Foam

3.6.1 EPS Storage Conditions Background

The post-molded EPS foam shrinkage behavior has been shown in prior studies dueto volatile matter content. EPS experiences steam condensation inside of its beads after steam chest molding and removed from the mold. Thus, inside the beads it has a lower pressure than the surrounding atmosphere which causes shrinkage [53]. After EPS demolding, the pressure and temperature of its environment decrease. This leads to the intra-cellular pressure decreasing to atmospheric pressure, and stiffening of the polystyrene material. Since PS is assumed to be viscoelastic for temperatures down to 20 °C and the secondary molecular transition that exist around 50° C, the residual pentane evaporation lead to separation of polymer chains, causing more free volume for molecular motion. This explains (less than 1%) small dimensional variations of EPS observed during after-shrinkage. A higher storage temperature after processing should then lead to faster after-shrinkage because shrinkage at a low final temperature is further from the dimension that is stable than shrinkage at a high final temperature [27]. Additionally, at room temperature, pentane diffusivity is independent of aging time for EPS. Increasing the temperature of storage, however, increases its dependence [29]. Thus, storing a portion of EPS plates, Group 2, were stored at a higher temperature to study the possibility of achieving faster shrinkage in this way. Dimensional testing was done to track this shrinkage of Group 2 plates, as well as Group 1A and 1B plates, in

order to see which group(s) reached stability according to the industry standard and what factors led to that stability.

3.6.2 Dimensional Testing

In order to track the shrinkage of the EPS plates, periodic dimensional measurements were taken. Only one of the three dimensions was measured because the material was assumed to be isotropic, thus exhibiting uniform shrinkage. Based on the assumption, the longest dimension was chosen for measurement in order to minimize error. Samples were measured dimensionally approximately one time per week. Measurements were taken at three points, as shown in *Figure 39* below, then averaged for each point of measurement.

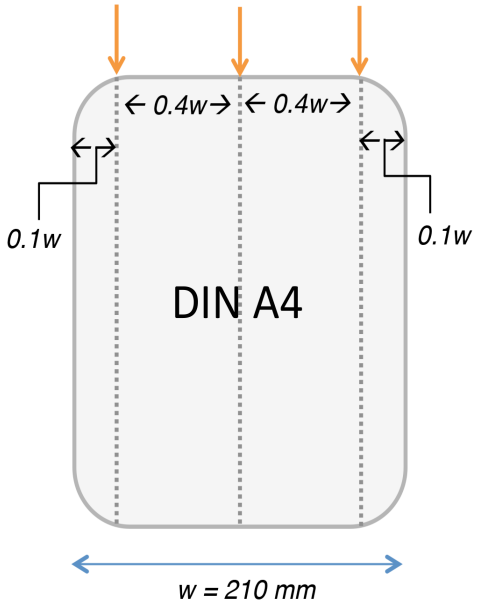

Figure 39: Dimensional testing three measurement points, which were then averaged each time to calculate the percent shrinkage. [Author]

Once the dimension at each of the three points shown in *Figure39* was measured each time, these values were averaged to calculate the dimension of the sample, like so:

$$l = \frac{1}{3}(l_1 + l_2 + l_3) \qquad \textit{(Equation 10)}$$

where l_1, l_2, and l_3 are the lengths measured at each of the three points. The accuracy of each measurement was 0.01 mm. To calculate the percent shrinkage, the measured length was compared to the mold length of 290 mm in the same dimension, using:

$$\%\, shrinkage = \frac{l_o - l}{l_o} \times 100 \qquad \textit{(Equation 11)}$$

Here, l_o is the mold length, equal to 290 mm for the EPS plates produced in this study. The percent shrinkage was averaged across all ten samples measured per group each day for Group 1A and Group 1B. For Group 2, after each incremental number of days of heating, three samples were removed from the high temperature oven and measured dimensionally continuously each week. For instance, those samples heated for 7 days in the oven were removed after one week, tested dimensionally, then stored at the 21 °C cellar for the remainder of the duration of the study with weekly dimensional measurements. Weekly measurements were taken of shrinkage in the longest dimension, since the material was assumed to be isotropic and thus exhibiting uniform shrinkage.

3.6.3 Dimensional Results

As pentane is a plasticizing blowing agent, it softens EPS at high temperature or low pressure to help with expansion. After expansion, the cells remain as soft bubbles with a slight vacuum inside. Thus, the cells must gradually be filled with air from the surrounding environment before EPS is strong and stable enough to be used. The shrinkage tracking of the samples done by dimensional measurements was used to determine what factors play a more prominent role in the shrinkage of EPS. Group 1A and 1B shrinkage history curves were compared to see if starting volatile matter content leads to faster shrinkage. Further, Group 1A and 2 samples were compared to determine if high temperature storage conditions play a more dominant role in EPS dimensional stability by affecting air diffusion into cells.

The shrinkage history of the Group 1A compared to Group 1B EPS plates is shown below, with shrinkage as a percentage (calculated with Equation 11) over time, expressed in days.

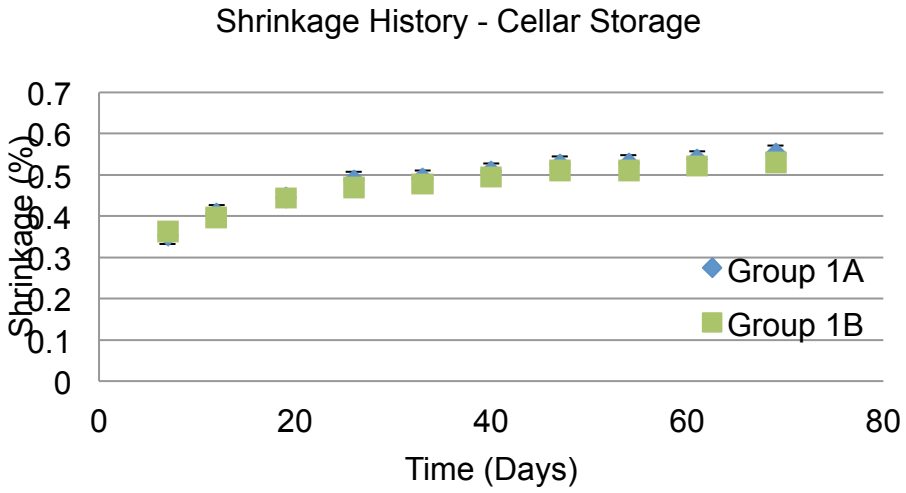

Figure 40: Shrinkage history of both 21 °C stored sample groups over time. The 0 point is taken as 24 hours after de-molding. [Author]

The graph in *Figure 40* outlines the differences in shrinkage rate with respect to time based on the amount of initial volatile matter in the microgranule raw material. The Group 1A plates had 4.61 wt% and the Group 1B samples had 4.08 wt% volatiles initially, as measured by TGA. The shrinkage is calculated as a percentage with respect to the design mold size of 290 mm in the measured direction, explained in Equation 11. Both groups follow a nearly identical shrinkage pattern, as outlined in the history graph, and both groups did not reach dimensional stability by the end of the duration of this study. 61 days after de-molding, the percent change in shrinkage of the Group 1A plates was approximately 0.046% compared to the point of measurement 28 days prior, and for Group 1B plates it was approximately 0.044%. Thus, the post-molding shrinkage of EPS does not vary greatly by the amount of volatiles initially present in the starting microgranule material.

The Group 2 samples were removed from the oven at incremental amounts of days and tested dimensionally to see if the amount of time spent in an elevated temperature (60 °C) affects stabilization time. This way, it could be determined how many days samples must be stored at a high temperature to achieve faster shrinkage. After they were removed from the high temperature, they were stored at 21 °C with the remaining Group 1A and Group 1B samples, and tested weekly dimensionally. The graph below outlines the differences in shrinkage rate with respect to the duration of time the Group 2 samples stored at 60° C, in comparison with the Group 1A plates stored at 21 °C.

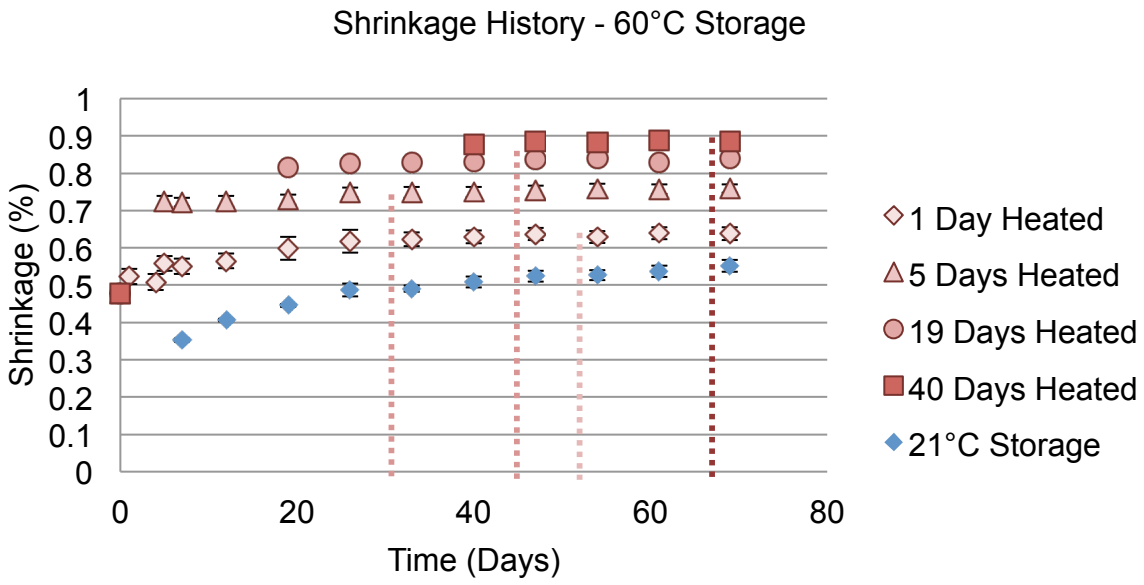

Figure 41: Shrinkage history of Group 2 compared with Group 1A. The point at which each Group 2 sample group reaches stability is also marked. [Author]

The starting point of the graph in *Figure 41* is taken as 24 hours after de-molding to allow for stabilization of the parts post-processing. The legend at the right shows the number of days each of the samples tested in Group 2 were heated in the oven before being removed and stored at 21 °C for the remainder of the duration of the trials. The shrinkage was calculated with respect to the designed mold size of 290 mm in the measured direction, following Equation 11. The graph shows two main points. First, it can be seen that Group 2 samples stored at a high temperature for a longer number of days reached a higher amount of shrinkage than those stored for fewer or no days in the oven. This could be due to the self-healing effect of the polymer chains, where a higher temperature for a longer amount of time leads to more self-healing and more space for molecules to diffuse out. It could also be due to the return of the polymer structure to its lowest energy state, thus minimizing entropy by coiling back into its original, pre-processed structure. However, as the focus of this study was the dimensional stability of EPS foam rather than its absolute amount of shrinkage reached, further detailed studies to explain this observation would be a possibility for future work. Second, all Group 2 samples stored at high temperature reached stability by the end of the duration of the trials. Samples heated for 5 days were fastest to reach stability, after 33 days after molding. Since all samples in Group 2 stored at 60 °C reached stability and neither sample Group 1A nor 1B reached stability, the high temperature storage temperature is a key determinant in EPS foam dimensional stability. The samples stored at 60 °C were in an environment that allowed for the stabilization of the pressure inside the foam beads by air diffusion into EPS. The high temperature increases the

kinetic energy of the air particles surrounding EPS samples, which increases their velocity. Therefore, air diffused faster into the foam cells to replace residual volatile matter, and the shrinkage of the plates was stabilized according to the industry standard.

Diffusion is a passive transport process of molecules moving from high to low concentration areas. The air molecules surrounding the samples move from high concentration in the ambient atmosphere to low concentration inside the cells. They must move through the hierarchy structure of the EPS foam structure as heavier molecules than the light volatile matter molecules that at the same time diffuse out of the material. Thus, the air takes longer to diffuse into the cells. Storing the plates at a higher temperature, however, increases the kinetic energy of the air particles surrounding the EPS plates, causing them to move at higher velocities. Thus, there is an increased rate of diffusion into the EPS cells to replace the volatile matter that diffuses out at a much higher rate. SEM imaging below also showed that cell sizes and inter-bead channels were approximately the same in both the 21 °C and 60 °C-stored samples. Thus, the only difference that high temperature storage provides is increased diffusion of air into the beads, which greatly decreases the time required for EPS plates to reach a point of dimensional stability.

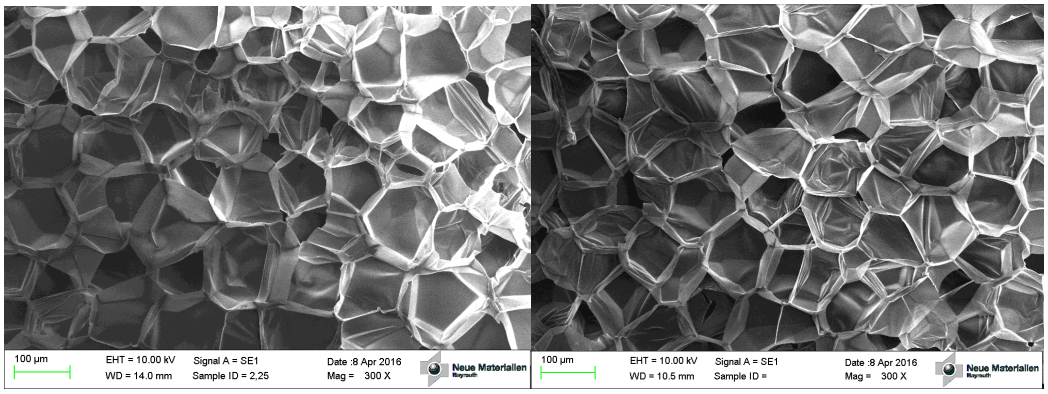

Figure 42: SEM imaging comparison of cell sizes in samples stored at 60 °C (left) and 21 °C (right). Both groups of samples can be seen to have approximately the same microstructural cell size. [Author]

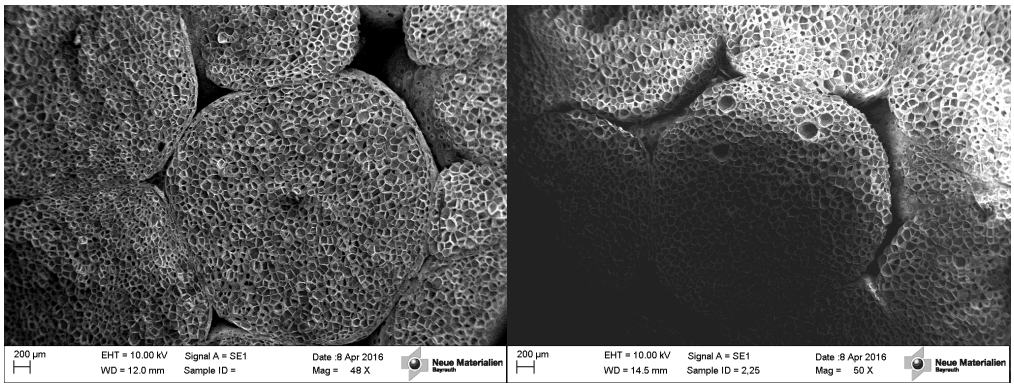

Figure 43: SEM imaging comparison of inter-bead channels in samples stored at 21 °C (left) and 60 °C (right). Both groups of samples can be seen to have approximately the same microstructural spacing between beads. [Author]

4 Summary and Outlook

The dimensional stability of post-processed expanded polystyrene foam was studied in this work. EPS used for building insulation must be defined as dimensionally stable by the industry standard before its use. Stability is normally reached within 11-18 weeks. This induces long storage times in warehouses after parts are produced before they can be used, making it costly due to its large volume of space consumption. There is therefore a great motivation to accelerate the shrinkage process of EPS foam to achieve faster dimensional stability.

To primarily examine material phase transitions and determine whether the polystyrene used in the materials in this study was semi-crystalline, DSC testing was performed on the two types of microgranules used in this study. This technique was chosen because if crystallization or melting temperature peaks were to be observed in the samples tested, it would indicate a portion of the polystyrene was crystalline. Thus, the crystallinity could effect diffusion of the volatile matter content out of the foam. The T_g was found to not vary too much between the two types of raw material, with a value of 95.2 °C for the “new” microgranules and 94.3 °C for the “old” beads. Additionally, the polystyrene was determined to be amorphous with no amounts of crystalline syndiotactic polystyrene, since no clear T_c or T_m peaks were found in the second heating curve from both groups of raw material beads.

The volatile matter content, polymer matrix residual stresses, and post-processed storage conditions of EPS were tested to determine their effects on shrinkage behavior. The same types of EPS foam, BASF Peripor 300E, was used to eliminate any possible material-caused behavior differences. This specific EPS material is highly used as building insulation, and thus the data produced in this study would be relevant to industry. The raw material microgranules were pre-foamed, then molded with steam-chest molding into plates of size DIN A4 with a thickness of 22 mm. Three groups of samples were studied to reveal the relationship between shrinkage compared to the materials' volatile matter content and storage conditions.

After EPS foam is processed, some of the pentane blowing agent remains within cells and can affect the shrinkage. To measure this volatile matter content at various points in its lifetime, TGA was used to regularly track the amount of volatiles as a weight percentage for samples from each of the three sample groups in this study. The "new" microgranules were determined to have a starting amount of 4.61 wt% volatiles, and the "old" beads had 4.08 wt%. All three sample groups reached a value of less than 1 wt% volatiles at approximately one week after de-molding; after this point, the volatile content appeared to no longer be dependent on the concentration.

GC-MS was also performed at different time in order to specify the composition of the volatile matter content within EPS. The purpose of this characterization technique was to determine if specific compounds within the volatile matter left in EPS foam affect dimensional stability more so than others. All samples were determined to have a

starting distribution of mostly n-pentane and approximately 10-15% isopentane for the volatile matter makeup in microgranule form. These two substances come from the blowing agent used to expand the microgranules into foam. Over time, samples from all three groups followed the same trend of a decrease in the amount of n-pentane with thus an increase in the fraction of volatiles being isopentane, since measurements were qualitative and thus relative. All groups ended with nearly the same distribution of volatiles, a clear majority of isopentane at the end of the trial period of 61 days after de-molding. The n-pentane fraction at this point was less than 5% of volatiles, if at all still remnant in the samples. However, only the oven-stored plates had reached stability according to the industry standard by the end of the trials. Thus, volatile matter content and amount was concluded to not be the final determinant of EPS shrinkage.

Residual stress testing was done with the hole drilling method as well as Raman spectroscopy to determine if either method would be possible for use with foams. As this type of testing has not been done with polymer foam materials before, the aim was to see if either method could reliably produce accurate residual stress values. Both methods, however, measured residual stress values with unknown accuracy. This could be either the result of not enough sensitivity with the instrumentation used for testing, or that EPS foam is a material with no significant residual stresses since it is made up of nearly entire air and the cell wall thicknesses are significantly lower than cell diameters. Thus, it could be concluded that current residual stress testing methods that were used

in this study would have to be further specialized to detect residual stresses in polymer foams.

The longest sample dimension length of samples from each of the three groups was also measured periodically over time in order to track their shrinkage profile. Both sample groups stored in the cellar did not reach stability in the 61 days after de-molding timeframe of this study. Group 1A samples had a difference of 0.046% shrinkage and Group 1B samples had a difference of 0.044% shrinkage at Day 61 compared to samples measured 28 days prior. All Group 2 high temperature storage samples, on the other hand, were stable by the end of the trials. The samples stored in the oven for 5 days reached stability by Day 33, with 0.02% difference in shrinkage compared to plates measured on Day 5. Thus, heating EPS at 60 °C for over 5 days would be costly and redundant to helping quicken shrinkage, since the 5 day storage already accomplishes swift stability in merely one month.

The microstructure of samples from each group was studied with SEM. Inter-bead channels and cell sizes were found to be approximately the same in both the oven- and cellar-stored samples. Therefore, the only difference in samples that achieved stability versus samples that did not were the high temperature storage conditions. Storing at a higher temperature allowed for quicker diffusion of the surrounding air into the foam beads, thereby stabilizing the cellular internal vacuum that arose after processing. The volatiles are lighter molecules with less mass than air, and thus diffuse out of the foam beads and creating space faster than air molecules have

the change to diffuse in. EPS thus shrinks until enough air has diffused into its beads to stabilize the cell internal vacuum. The high temperature storage of Group 2 samples allowed for air to diffuse quickly into the parts, decreasing the vacuum inside cells and leading to fast dimensional stabilization in accordance with DIN EN 1603.

This thesis showed that air diffusion into the cells after de-molding is key to EPS stability. It stabilizes the internal vacuum caused by the liquefaction of the blowing agent being exposed to a lower temperature after processing. This air diffusion plays a significant role in the dimensional stability of EPS foam in addition to volatile matter from the blowing agent that diffuses out. The residual stress contribution to dimensional stability, however, is still not entirely clear, and would be interesting to pursue. Modifying current measurement methods in order to detect stresses in foams made up of mostly air, as well as developing more standardized and automated ways for measuring with the curvature layer removal method could lead to a better understanding of the polymer matrix behavior in EPS shrinkage. Additionally, finding means to measure the pressure inside of cells would compliment in greater detail the work done in this study. The air diffusion into the beads was found to have a very significant and long-term role in accelerating the reaching of the material's dimensional stability. Hence, as a result of the findings in this work, a shift in focus of EPS dimensional stability studies to quicken air diffusion into the cells rather than volatile matter diffusion out of the material is encouraged.

References

[1] "Chapter 21: The Solid State of Matter." *OpenStax CNX*. UT Austin - Principles of Chemistry I, n.d. Web.

[2] "Differential Scanning Calorimetry." *Polymer Science Learning Center*. The University of Southern Mississippi - Department of Polymer Science, 2005. Web.

[3] "Expandable Polystyrene Market: Global Industry Analysis and Opportunity Assessment 2014 - 2020." *Expandable Polystyrene Market: Global Industry Analysis and Opportunity Assessment 2014 - 2020*. Future Market Insights, 2014. Web.

[4] "Glass-Rubber Transition." Sahand Univ of Technology - Department of Polymer Engineering, Tabriz, Iran. Web.

[5] "Global Expanded Polystyrene (EPS) Market Segmented by Application and Geography Trends and Forecasts (2015-2020) - Reportlinker Review." *PR Newswire*. Reportlinker, 17 Sept. 2015. Web.

[6] "Polymer Foams Market Expected to Consume 25.3 Million Tonnes by 2019." *Smithers RAPRA*. Smithers Group, n.d. Web.

[7] "Polystyrene, EPS Markets Expect Growth." *Plastics Decorating*. N.p., 2016. Web.

[8] "Polystyrene." *Polymer Science Learning Center*. The University of Southern Mississippi - Department of Polymer Science, 2005. Web.

[9] "QII HERS Credit Now Allows Open Cell Spray Foam." *Green Compliance Plus*. N.p., n.d. Web.

[10] "Residual Stress." *U of M: Department of Mechanical Engineering*. University of Minnesota Twin Cities, n.d. Web.

[11] "What Is Thermal Insulating System?" *JAB Deluxe Decorating*. Design Solutions, n.d. Web.

[12] Altstädt, Volker. "Polymer Foams." Polymere 2. University of Bayreuth - Department of Polymer Engineering, Bayreuth, Germany. 23 Apr. 2015. Lecture.

[13] Andersen, Roy. *EPS Geofoam Blocks, Material Properties and Production Processes*. Rep. Jackson AS, Norway: n.p., n.d. Web.

[14] BASF. "Spezialschäume – Technische Schäume." Web.

[15] Bhide, Shreyas Y., and S. Yashonath. "N -Pentane and Isopentane in One-Dimensional Channels." *J. Am. Chem. Soc. Journal of the American Chemical Society* 125.24 (2003): 7425-434. *JACS Articles*. Web.

[16] Booth, J.R., and T.J. Holstein. "Determination of Effective Diffusion Coefficients of Nitrogen in Extruded Polystyrene Foam by Gravimetric Sorption." *Journal of Building Physics* 16.3 (1993): 246-62. Web.

[17] Colton, Jonathan S., and Nam P. Suh. "Nucleation of Microcellular Foam: Theory and Practice." *Polym. Eng. Sci. Polymer Engineering and Science* 27.7 (1987): 500-03. Web.

[18] *Dan Gardner Drywall Co.* N.p., n.d. Web.

[19] Dhingra, Sukhtej Singh. "Mixed Gas Transport Study through Polymeric Membranes: A Novel Technique." Thesis. Virginia Polytechnic Institute and State University, 1997. Web.

[20] *Differential Scanning Calorimetry of Polystyrene*. Socorro, New Mexico: New Mexico Institute of Mining and Technology - Physical Chemistry I Laboratory, n.d. PDF.

[21] *Differential Scanning Calorimetry; First and Second Order Transitions in PETE*. Waterville, Maine: Colby University - Department of Chemistry, n.d. PDF.

[22] Downes, Andrew, and Alistair Elfick. "Raman Spectroscopy and Related Techniques in Biomedicine." *Sensors* 10.3 (2010): 1871-889. Web.

[23] Eupe, M. P. I. M., and P. C. Powell. "A Modified Layer Removal Analysis for the Determination of Internal Stresses in Polymer Composites." *Journal of Thermoplastic Composite Materials* 10.4 (1997): 334-52. *SAGE Social Science Collections*. Web.

[24] *Expanded Polystyrene (EPS) and the Environment*. Rep. EPS Packaging Group, n.d. Web.

[25] *Expanded Polystyrene Storage and Handling Safety Guide*. Rep. NOVA Chemicals Corporation, 2005. Web.

[26] Felder, R. M., R. D. Spence, and J. K. Ferrell. "A Method for the Dynamic Measurement of Diffusivities of Gases in Polymers." *Journal of Applied Polymer Science J. Appl. Polym. Sci.* 19.12 (1975): 3193-200. Web.

[27] Fen-Chong, Teddy, Eveline Hervé, and André Zaoui. "Micromechanical Modelling of Intracellular Pressure-induced Viscoelastic Shrinkage of Foams: Application to Expanded Polystyrene." *European Journal of Mechanics - A/Solids* 18.2 (1999): 201-18. *Elsevier, Paris*. Web.

[28] Fen-Chong, Teddy, Éveline Hervé, André Dubault, and Jean Louis Halary. "Viscoelastic Characteristics of Pentane-swollen Polystyrene Beads." *Journal of Applied Polymer Science J. Appl. Polym. Sci.* 73.12 (1999): 2463-472. Web.

[29] Fossey, D. J., and C. H. Smith. "Determination of the Diffusivity of N-pentane in Polystyrene Bead Foam." *Journal of Applied Polymer Science J. Appl. Polym. Sci.* 17.6 (1973): 1749-770. Web.

[30] Hajova, Hana, Josef Chmelar, Andra Nistor, Tomas Gregor, and Juraj Kosek. "Experimental Study of Sorption and Diffusion of N -Pentane in Polystyrene." *Journal of Chemical & Engineering Data J. Chem. Eng. Data* 58.4 (2013): 851-65. *ACS Publications*. Web.

[31] *How Foam Expands – Change of Properties Due to Several Parameters*. N.p.: StyroChem, n.d. PPT.

[32] *ISO 2796: Cellular Plastics, Rigid - Test for Dimensional Stability*. N.p.: International Organization for Standardization (ISO), 1986. PDF.

[33] Kandil, F. A., J. D. Lord, and P. V. Grant. *A Review of Residual Stress Measurement Methods - A Guide to Technique Selection*. Rep. no. ISSN 1473-2734. Middlesex, UK: NPL Materals Centre, 2001. Web.

[34] Kannan, P., J. J. Biernacki, D. P. Visco, J. Dunne, A. Mether, and D. Kirby. "Gas Diffusivity Through EPS Foams." *Journal of Cellular Plastics* 46.4 (2010): 353-73. Web.

[35] Klempner, Daniel, and Vahid Sendijarevic. *Handbook of Polymeric Foams and Foam Technology: Daniel Klempner and Vahid Sendijarevic*. 2nd ed. Munich: Hanser Gardner Publications, 2004. Print.

[36] Kundra, Pawan, Simant R. Upreti, Ali Lohi, and Jiangning Wu. "Experimental Determination of Composition-Dependent Diffusivity of Carbon Dioxide in Polypropylene." *Journal of Chemical & Engineering Data J. Chem. Eng. Data* 56.1 (2011): 21-26. Web.

[37] Kusch, Peter, and Gerd Knupp. "Analysis of Residual Styrene Monomer and Other Volatile Organic Compounds in Expanded Polystyrene by Headspace Solid-phase Microextraction Followed by Gas Chromatography and Gas Chromatography/mass Spectrometry." *J. Sep. Science Journal of Separation Science* 25.8 (2002): 539-42. *ResearchGate*. Web.

[38] Laurindo, João B., and Micha Peleg. "Mechanical Measurements In Puffed Rice Cakes." *Journal of Texture Studies J Texture Studies* 38.5 (2007): 619-34. Web.

[39] Lee, Eung Kee (Richard). *Novel Manufacturing Processes for Polymer Bead Foams*. Thesis. University of Toronto, 2010. Web.

[40] Malewska, Elzbieta, and Aleksander Prociak. "Modification of Expandable Polystyrene Beads." *Technical Transactions - Chemistry* (2015): 77-87. Web.

[41] Maul, Jürgen, Bruce G. Frushour, Jeffrey R. Kontoff, Herbert Eichenauer, and Karl-Heinz Ott. "Polystyrene and Styrene Copolymers." *Ullmann's Encyclopedia of Industrial Chemistry* 29 (2000): 475-522. Web.

[42] Maxwell, A. S. *Measurement of Residual Stress in Plastics*. Rep. Process Materials - National Physical Laboratory, 2005. Web.

[43] Mills, N.j., R. Stämpfli, F. Marone, and P.a. Brühwiler. "Finite Element Micromechanics Model of Impact Compression of Closed-cell Polymer Foams." *International Journal of Solids and Structures* 46.3-4 (2009): 677-97. *Elsevier*. Web.

[44] Mills, Nigel. *Polymer Foams Handbook: Engineering and Biomechanics Applications and Design Guide*. 1st ed. Oxford: Butterworth Heinemann, 2007. Print.

[45] Miltz, Joseph, and Ori Ramon. "Characterization of Stress Relaxation Curves of Plastic Foams." *Polym. Eng. Sci. Polymer Engineering and Science* 26.19 (1986): 1305-309. Web.

[46] National Center for Biotechnology Information. PubChem Compound Database; CID=7406, https://pubchem.ncbi.nlm.nih.gov/compound/7406.

[47] National Center for Biotechnology Information. PubChem Compound Database; CID=3776, https://pubchem.ncbi.nlm.nih.gov/compound/3776.

[48] National Center for Biotechnology Information. PubChem Compound Database; CID=7410, https://pubchem.ncbi.nlm.nih.gov/compound/7410.

[49] Olivero-Verbel, Jesus, Nerlis Pajaro-Castro, and Karina Caballero-Gallardo. "Identification of Volatile Organic Compounds (VOCs) in Plastic Products Using Gas Chromatography and Mass Spectrometry (GC/MS)." *Ambiente & Agua - An Interdisciplinary Journal of Applied Science* 9.4 (2014): 610-20. Web.

[50] *Particle Foam 2015*. Düsseldorf: VDI Verlag GmbH, 2015. Print.

[51] *Peripor 300E Safety Data Sheet*. N.p.: BASF, 12 Aug. 2014. PDF.

[52] *Raman Spectroscopy Basics*. N.p.: Princeton Instruments, n.d. PDF.

[53] Raps, Daniel, Nemat Hossieny, Chul B. Park, and Volker Altstädt. "Past and Present Developments in Polymer Bead Foams and Bead Foaming Technology." *Polymer* 56 (2015): 5-19. *Elsevier*. Web.

[54] *Residual Stress Measurement Based on Hole-drilling and ESPI*. N.p.: Stresstech Group, n.d. PDF.

[55] Schajer, Gary S. *Advances in Hole-drilling Residual Stress Measurements*. Proc. of XIth International Congress and Exposition, Orlando, FL. N.p.: Society for Experimental Mechanics, 2008. Print.

[56] Schajer, Gary S., and Michael Steinzig. "Full-field Calculation of Hole Drilling Residual Stresses from Electronic Speckle Pattern Interferometry Data." *Experimental Mechanics* 45.6 (2005): 526-32. Web.

[57] Schajer, Gary S., and Michael Steinzig. *Dual-axis Hole-drilling ESPI Residual Stress Measurements*. Proc. of Denver X-ray Conference (DXC), Denver, CO. N.p.: JCPDS - International Centre for Diffraction Data, 2009. 633-42. Print.

[58] Shutov, Fedor A. *Integral/structural Polymer Foams: Technology, Properties, and Applications*. 1st ed. Berlin: Springer-Verlag Berlin Heidelberg GmbH, 1985. Print.

[59] Singh, Sachchida N., Monica Nitru-Karamagi, and Michael Ritchie. *Optimizing Polyiso Blowing Agents*. Rep. Huntsman Advanced Technology Center, n.d. Web.

[60] *Standard Test Method for Determining Residual Stresses by the Hole-Drilling Strain- Gage Method*. West Conshocken, PA: commod, n.d. PDF.

[61] *Technopol SA Energy Saving Materials*. N.p., n.d. Web.

[62] *Thermal Insulating Products for Building Applications - Determination of Dimensional Stability under Constant Normal Laboratory Conditions*. N.p.: DIN Standards Committee Building and Civil Engineering, 2013. PDF.

[63] Tomba, J. Pablo, José M. Carella, David García, and José M. Pastor. "Liquid−Liquid Limited-Supply Diffusion Studies in the Polystyrene−Poly(vinyl Methyl Ether) Pair." *Polymer* 43 (2002): 6751-760. *Elsevier*. Web.

[64] Trassl, C., and V. Altstädt. "Particle Foams: Future Materials for Lightweight Construction and Design." *Kunststoffe International* 2 (2014): 73-76. Web.

[65] Tuladhar, T.r., and M.r. Mackley. "Experimental Observations and Modelling Relating to Foaming and Bubble Growth from Pentane Loaded Polystyrene Melts." *Chemical Engineering Science* 59.24 (2004): 5997-6014. *Elsevier*. Web.

[66] Turnbull, A., A. S. Maxwell, and S. Pillai. "Residual Stress in Polymers—Evaluation of Measurement Techniques." *Journal of Materials Science* 34 (1999): 451-59. *Kluwer Academic Publishers*. Web.

[67] Verlag, Carl Hanser. *Expandable Polystyrene (EPS)*. Rep. Munich, Germany: Kunstoffe, 2005. *Commodity Plastics*. Web.

[68] Verlag, Carl Hanser. *Expandable Polystyrene (EPS)*. Rep. Munich, Germany: Kunstoffe, 2011. *Commodity Plastics*. Web.

[69] Verlag, Carl Hanser. *Rigid Polystyrene Foam (EPS, XPS)*. Rep. no. PE110869. Munich, Germany: Kunstoffe International, 2011. Web.

[70] Walker, Donna. "Residual Stress Measurement Techniques." *Advanced Materials & Processes* (2001): 30-33. Web.

[71] Winterling, H., and N. Sonntag. "Polystyrene Foam (expanded Polystyrene, EPS)." *Kunststoffe International* 101.10 (2011): 18-21. Web.

[72] Zhang, Q., M. Xanthos, and S. K. Dey. "Parameters Affecting the In-Line Measurement of Gas Solubility in Thermoplastic Melts during Foam Extrusion." *Journal of Cellular Plastics* 37.4 (2001): 284